

# Towards the Vision-Sound-Language-Action Paradigm: The HEAR Framework for Sound-Centric Manipulation

Journal Title  
XX(X):1–29  
©The Author(s) 0000  
Reprints and permission:  
sagepub.co.uk/journalsPermissions.nav  
DOI: 10.1177/ToBeAssigned  
www.sagepub.com/

SAGE

Chang Nie<sup>1</sup>, Tianchen Deng<sup>1</sup>, Guangming Wang<sup>2</sup>, Zhe Liu<sup>1</sup> and Hesheng Wang<sup>1</sup>

## Abstract

Humans and animals rely on the seamless integration of continuous visual and auditory streams to interact with the physical world. While recent Vision-Language-Action (VLA) models have begun to incorporate audio, they typically treat sound as static pre-execution prompts or focus exclusively on human speech. This leaves a significant gap in real-time, sound-centric manipulation where fleeting environmental acoustics (e.g., a microwave beep or a collision click) provide critical state verification during the actual execution of a task. A primary challenge in utilizing continuous audio lies in its temporal nature. Unlike visual scenes, which usually change gradually and remain observable across control steps, acoustic cues are fleeting. Because of this transience, key sounds can easily be missed due to low-frequency policy updates or system latency. This problem is exacerbated by action chunking with open-loop execution, which creates a Blind Execution Interval where important acoustic events are lost between discrete audio observation windows. Recognizing the necessity of continuous auditory awareness, we formalize Vision-Sound-Language-Action (VSLA) as a novel continuous control paradigm conditioned on vision, streaming audio, language instructions, and proprioception under delayed decision loops. As a concrete instantiation, we introduce HEAR, a VSLA framework that integrates four components: (i) a streaming *Historizer* designed to maintain a compact, causal audio context across execution gaps; (ii) an *Envisioner* adapted from omni foundation models to reason over integrated multi-sensory inputs; (iii) an *Advancer*, formulated as an audio world model, to learn temporal dynamics by predicting near-future audio codes; and (iv) a flow-matching *Realizer* policy constructed to generate smooth action chunks. To address the scarcity of pretraining data and standardized evaluations for VSLA, we construct OpenX-Sound for pretraining, alongside HEAR-Bench, the first sound-centric manipulation benchmark with strict causal timing rules. Extensive evaluations on HEAR-Bench demonstrate that HEAR achieves an average success rate of 81% in simulation, significantly outperforming waveform rendering (61%) and an ASR baseline (35%). Furthermore, HEAR promising real-world performance in real-world deployments, achieving a 54% success rate across four sound-centric tasks on a physical Franka Panda robot. Our results suggest that robust sound-centric manipulation necessitates causal persistence and explicit temporal learning. We believe this framework provides a practical step toward multi-sensory foundation models for embodied agents, enabling robots to more comprehensively perceive and interact with dynamic environments. Code and videos are available at <https://hear.irmv.top>.

## Keywords

Vision-Language-Action (VLA), robot learning, sound-centric manipulation, auditory processing, multimodal learning, action chunking

## 1 Introduction

In natural evolution, auditory perception did not emerge solely for communication. It evolved as a primal mechanism for organisms to monitor and manipulate their physical surroundings (Stein and Meredith 1993). While vision captures precise spatial geometry and has been extensively

<sup>1</sup>School of Automation and Intelligent Sensing, Shanghai Jiao Tong University and Shanghai Key Laboratory of Navigation and Location Based Services, Shanghai 200240, China

<sup>2</sup>Department of Engineering, Cambridge University, Cambridge, CB2 1TN, UK

modeled through advanced 3D representations and visual foundation models (Deng et al. 2025, 2024), sound provides a continuous, omnidirectional stream of temporal events. Ambient acoustics and contact noises reveal critical physical states that cameras simply cannot see, from the subtle sputtering of boiling liquid to the sharp click of objects colliding. Current Vision-Language-Action (VLA) models, such as Octo (Team et al. 2024), OpenVLA (Kim et al. 2024), and  $\pi_{0.5}$  (Intelligence et al. 2025), have proven highly effective at mapping visual snapshots and text instructions directly to continuous control. However, these foundational systems operate in a fundamentally silent world. Recognizing this limitation, recent pioneering works have sought to introduce audio into robotic manipulation. Some practical methods incorporate sound by transcribing human speech into text prompts via automatic speech recognition (Radford et al. 2023) or by rendering short audio waveforms as static 2D images (Gong et al. 2021). More recently, advanced multisensory models, such as OmniVLA (Guo et al. 2025) and Audio-VLA (Wei et al. 2025), have begun projecting audio into shared representation spaces to enhance instruction understanding and intent inference.

Despite these significant strides, a structural limitation remains: most existing approaches process audio in a highly episodic or static manner. They are primarily designed to listen before acting—using sound to establish context, disambiguate objects, or receive verbal commands prior to movement. While highly effective for high-level reasoning, these methods struggle to utilize sound as a continuous, real-time feedback signal during physical interaction. Because their architectures do not treat audio as an ongoing sensory stream, they remain oblivious to the rich, non-verbal acoustic dynamics (such as a sudden collision click or a fleeting machine beep) that unfold irregularly during task execution. To achieve robust physical intelligence, robots must be empowered not just to hear instructions before moving, but to actively listen while acting.

To systematically leverage this acoustic environment in robotic manipulation, we categorize everyday audio cues into four primary types: speech sound, event-triggered sound, continuous process sound, and physical interaction feedback. While speech primarily provides high-level direction, the latter three offer critical low-level state information. Most notably, physical interaction feedback, such as the distinct acoustics of collisions, can serve as a pervasive and low-cost surrogate for expensive tactile sensors (Sinapov et al. 2009; Huang et al. 2025). However, harnessing these rich acoustic cues poses a severe challenge for real-world control

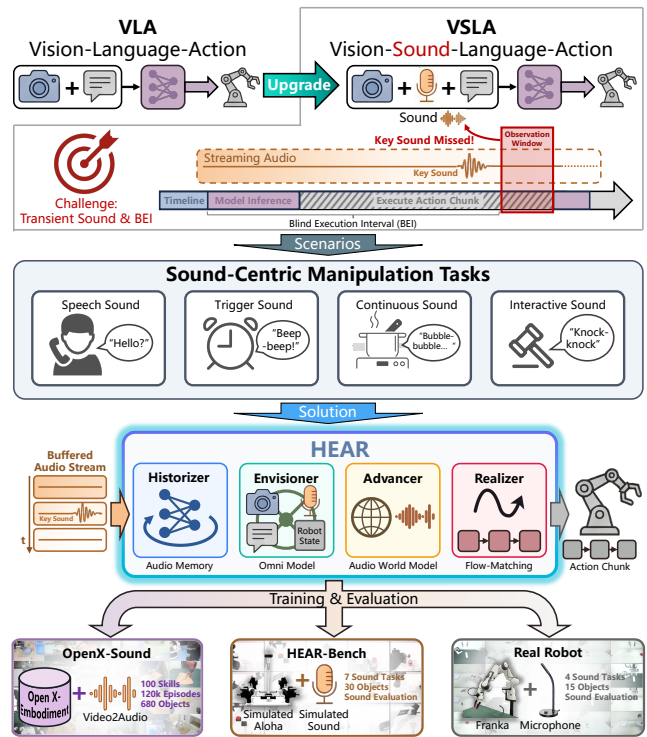


**Figure 1. The HEAR framework for**

**Vision-Sound-Language-Action (VSLA) manipulation.**

**Challenge:** Upgrading standard VLA to the VSLA paradigm.

We highlight a critical challenge: VLA models frequently miss transient acoustic cues due to the Blind Execution Interval (BEI), a structural blind spot caused by system latency and open-loop action chunking. **Scenarios:** Everyday sound-centric manipulation tasks require robots to perceive diverse acoustic cues, including speech, trigger, continuous, and interactive sounds. **Solution:** To address the BEI and handle complex sounds, the HEAR framework integrates four components: a causal audio memory (*Historizer*), an omni-sensory reasoning model (*Envisioner*), a predictive audio world model (*Advancer*), and a smooth flow-matching policy (*Realizer*). **Training & Evaluation:** We introduce *OpenX-Sound* for scalable pretraining, alongside *HEAR-Bench* and physical robot deployments for rigorous, sound-causal evaluation.

due to their inherently transient nature. Unlike visual states that typically persist in the camera’s field of view, sound-centric tasks usually hinge on brief, non-repeatable events like a microwave “ding” or an impact “tap”. Due to inherent computational and mechanical latencies, real-world robot systems cannot process sensory inputs continuously. Instead, they are forced to acquire data in discrete intervals, creating structural blind spots where fleeting environmental signals are easily missed. This over-reliance on persistent vision often causes the robot to violate the fundamental causal logic of the task. For instance, a policy might prematurely

**Corresponding author:**

Hesheng Wang, School of Automation and Intelligent Sensing, Shanghai Jiao Tong University and Shanghai Key Laboratory of Navigation and Location Based Services, Shanghai 200240, China.

Email: wanghesheng@sjtu.edu.cn

execute an action that must strictly occur only *after* a specific auditory trigger.

Although resolving this temporal blind spot is essential for robust control, incorporating streaming audio into modern VLA pipelines remains structurally difficult. Most existing approaches attempt to circumvent this issue through rigid, windowed adapters. For instance, Automatic Speech Recognition (ASR) modules transcribe audio and append the text to the language prompt (Baevski et al. 2020; Radford et al. 2023), while visual adapter methods plot a short audio waveform into a 2D image, treating it as an additional “camera view” (Gong et al. 2021). These adapters can succeed when cues are prolonged and well-aligned with the observation window. However, they inherently lack temporal persistence and cannot represent that a brief event occurred just before the current window. Furthermore, these representations degrade the original signal. ASR discards vital non-speech cues and prosody. Rendering a waveform as an image captures amplitude changes but completely obscures rich spectral details and frequency contours. Ultimately, these adapters struggle because they force dynamic audio streams into static, vision-like snapshots.

A primary distinction between these modalities lies in how their information is distributed over time. We acknowledge that in highly dynamic tasks, such as catching flying objects (Kim et al. 2014), visual states can also be highly transient. However, in the context of everyday manipulation, the visual scene usually changes gradually because physical objects and robot arms move at limited speeds. Even when the robot is holding still, the camera provides a steady, information-rich observation of the environment. Because objects generally remain in the camera’s view, visual perception is highly forgiving to minor system delays.

Audio exhibits the exact opposite pattern. During steady periods, the acoustic environment mostly consists of low-information background noise. Critical physical information is heavily concentrated in brief, transient moments, such as the sudden click of a collision or the short beep of a microwave. An acoustic cue lasting merely 50 to 200 milliseconds is irreversibly lost if the policy is not actively listening at that exact moment. Therefore, while a brief system delay only makes a visual observation slightly outdated, the same delay can cause the robot to miss a crucial sound entirely, leading to catastrophic task failures.

Modern large-model policies exacerbate this vulnerability. Because their heavy computation prevents them from running at the robot’s high control frequency, many VLA systems rely on action chunking (Zhao et al. 2023) to maintain smooth continuous motion. In this paradigm, the

policy predicts a short sequence of actions and executes them in an open-loop manner. This creates a hard execution gap that we term the Blind Execution Interval (BEI). During this interval, the robot is effectively oblivious to new observations, causing it to easily miss short-lived acoustic cues. An intuitive solution to this problem might be to increase the replanning frequency or to interrupt the open-loop execution early. However, such naive interruptions not only introduce discontinuous, jerky motion, but also frequently trap the robot in localized, repetitive action loops, severely degrading execution quality. Furthermore, even if the replanning frequency is pushed to its limit, the inherent end-to-end system latency ensures that fleeting acoustic events will still fall outside the boundaries of a rigid observation window. Therefore, the fundamental bottleneck is not merely a delayed physical reaction, but the irreversible loss of critical sensory information. We identify this structural data loss as the first major challenge in audio-driven control.

A second challenge lies in temporal perception and action generation. Beyond successfully capturing a fleeting sound, the policy must also translate this cue into an appropriate physical response. Sound-centric tasks typically require a robot to hold steady and listen, followed by an immediate reaction to an acoustic trigger. Because modern VLA models often rely on single-frame observations without an explicit representation of time, they struggle to model this behavior. When operating over long horizons, these policies frequently suffer from Temporal Motion Collapse (Zhao et al. 2023), where meaningful movements concentrate early in an action chunk while later steps degenerate. Without proper temporal grounding, the robot tends to drift or freeze instead of maintaining a stable listening posture, which prevents the immediate reaction required for audio-driven tasks.

To systematically address these structural bottlenecks, we formalize **Vision–Sound–Language–Action (VSLA)** as a novel continuous control paradigm. This paradigm is conditioned on multi-view vision, streaming audio, language instructions, and robot proprioception, operating under realistic constraints of delayed, low-rate, and asynchronous policy updates. While VSLA establishes the overarching theoretical goal of continuous auditory awareness, translating it into real-world control requires concrete architectural innovations. To instantiate this paradigm, we propose **HEAR**, an end-to-end framework designed to fundamentally decouple high-frequency sensory memory from low-frequency decision-making, as outlined in Figure 1. HEAR comprises four deeply integrated components: First, to eliminate the Blind Execution

Interval (Challenge 1), the streaming **Historizer** maintains a compact, causal audio context across execution gaps, ensuring that fleeting sounds are captured regardless of the policy query rate. Second, the **Envisioner**, a tailored omni foundation model, reasons over this newly integrated sensory context to extract actionable representations. Third, to resolve Temporal Motion Collapse (Challenge 2), we introduce the **Advancer**, an audio world model that explicitly predicts near-future audio codes, learning temporal dynamics and grounding the policy in a continuous flow of time. Finally, the flow-matching **Realizer** policy translates these representations into smooth, continuous joint-position action chunks.

Beyond algorithmic design, the broader field of audio-driven robotics is bottlenecked by a severe scarcity of synchronized data and rigorous evaluation platforms. To unlock large-scale pretraining for sound-centric manipulation, we introduce OpenX-Sound. This dataset transforms existing Open X-Embodiment episodes by augmenting them with synchronized audio tracks, which are generated via advanced video-to-audio generation models (Luo et al. 2023; Liu et al. 2024a). More importantly, to facilitate fair and standardized evaluation of the VSLA paradigm, we develop a novel real-time audio-physics co-simulation engine. Built upon this engine, we establish HEAR-Bench. Unlike standard visual simulators that remain completely silent, HEAR-Bench explicitly evaluates true auditory reactivity. It enforces causally strict success rules that actively reject visually plausible but premature actions. Specifically, if a robot relies solely on visual cues to initiate or complete a task before the required audio trigger occurs, the execution is strictly classified as a failure. This rigorous design ensures that policies are judged on genuine acoustic responsiveness rather than visual memorization or spurious correlations.

We thoroughly validate our approach across this new benchmark and multiple physical robot setups. In both simulated and real-world environments, HEAR substantially outperforms traditional ASR and waveform-adapted baselines. The performance improvements are particularly pronounced in tasks that rely on brief non-speech triggers and long-horizon process monitoring. These are precisely the settings where rigid windowed interfaces become brittle and fail. Ultimately, our results underscore a fundamental systems-level lesson: robust sound-centric manipulation cannot be achieved by merely appending an audio input stream to existing models. Instead, it demands continuous causal persistence and explicit temporal grounding. By introducing the VSLA paradigm alongside OpenX-Sound and HEAR-Bench, this research provides

the necessary tools to move past traditional vision-only policies, ultimately advancing the development of multi-sensory embodied agents.

Our primary contributions are summarized as follows:

- **The VSLA Paradigm & Structural Bottlenecks:** We formalize the *Vision–Sound–Language–Action* (VSLA) paradigm to extend current VLA policies with continuous auditory awareness. In pursuing this, we identify a fundamental obstacle: the *Blind Execution Interval* (BEI), a structural vulnerability where system latency and open-loop chunking render transient audio irrecoverable for standard memoryless systems.
- **The HEAR Framework:** To overcome this bottleneck and concretely instantiate VSLA, we propose **HEAR**, a novel end-to-end continuous control architecture. It ensures causal persistence and temporal grounding via four integrated components: a streaming causal audio memory (*Historizer*), multimodal reasoning (*Envisioner*), predictive audio dynamics (*Advancer*), and smooth flow-matching action generation (*Realizer*).
- **Datasets, Benchmark, & Experiments:** We introduce **OpenX-Sound** for large-scale pretraining. Furthermore, to facilitate rigorous and standardized evaluation, we develop a real-time audio-physics co-simulation engine to establish **HEAR-Bench**, the first benchmark explicitly designed for sound-causal manipulation. Extensive simulated and real-world deployments demonstrate that HEAR significantly outperforms baselines in genuine acoustic reactivity.

## 2 Related Work

### 2.1 Vision–Language–Action Policies

Recent advancements in robot learning have demonstrated the effectiveness of VLA policies. Earlier systems frequently used large language models to plan high-level steps while leaving low-level control to separate modules (Ahn et al. 2023; Huang et al. 2023). The current trend has moved toward end-to-end models that map language instructions and camera images directly to continuous robot actions (Brohan et al. 2023; Zitkovich et al. 2023; Driess et al. 2023; Nie et al. 2025). Supported by large datasets like Open X-Embodiment (O’Neill et al. 2024), models such as Octo (Team et al. 2024) and OpenVLA (Kim et al. 2024) have achieved strong performance across different robot platforms. Crucially, the entire architecture of these modern VLAs is tailored for visual data. Because visual scenes typically change smoothly and objects remain in the

camera’s view over time, these models can safely rely on discrete image snapshots taken at a relatively low frequency.

To manage the heavy computation of these large models and ensure smooth robot movement, most VLA systems incorporate action chunking (Zhao et al. 2023). Instead of predicting one step at a time, the policy generates a short sequence of actions and executes them without waiting for new sensor updates. This approach has been widely adopted and improved by generative models like Diffusion Policy (Chi et al. 2025) and flow-matching methods such as  $\pi_{0.5}$  (Intelligence et al. 2025; Lipman et al. 2023). While this open-loop execution effectively hides computation delay, it creates a temporary gap in perception, which we refer to as the Blind Execution Interval (BEI).

For purely visual tasks, the BEI is usually manageable because the visual state persists across the execution gap. However, this architectural design becomes a significant bottleneck when researchers attempt to incorporate highly transient signals like audio. A brief acoustic trigger, such as a click, can easily occur and finish while the robot is executing an action chunk. When the next observation window finally opens, the sound is already gone. Therefore, extending current VLA models to sound-centric tasks requires new mechanisms to maintain continuous sensory memory across these execution gaps. Our work builds upon the continuous control capabilities of existing flow-matching models but specifically addresses this timing mismatch to ensure fleeting sounds are not lost.

## 2.2 Audio in Robotics

Audio has historically played a variety of roles in robotics, ranging from high-level human interaction to low-level physical feedback. For high-level tasks, audio has traditionally been treated as a communication channel. Many systems utilize automatic speech recognition (ASR) modules (Baevski et al. 2020; Radford et al. 2023) to convert spoken commands into text prompts. Recent advancements have sought to integrate speech more directly into VLA models. For example, frameworks like SVA and VLAS explicitly process speech instructions to retain speaker identity and prosody, which are otherwise lost in pure text transcription (Li et al. 2025; Zhao et al. 2025). While highly effective for human-robot interaction, these methods primarily focus on explicit verbal commands rather than the ambient acoustic physics generated during manipulation. In the domain of navigation, agents frequently use sound to localize sources or infer off-screen events (Chen et al. 2020). However, navigation agents can typically move their base to improve listening geometry over time, whereas manipulation requires

reacting to brief temporal events exactly when the robot is generating significant mechanical ego-noise.

Beyond direct commands, recent works have explored audio for broader instruction understanding and proactive intent inference. For instance, audio-visual models can utilize sound to disambiguate visually identical objects when language commands are otherwise unclear (Guo et al. 2023). Notably, RoboOmni (Wang et al. 2025b) studies proactive manipulation within an omni-modal context, where a robot infers human intent by combining dialogue with environmental sounds. While these approaches represent a significant step toward multi-sensory intelligence, they primarily utilize audio to establish context or infer intent prior to, or around, the execution of an action. They generally do not treat audio as a low-level, real-time physical feedback signal during contact, nor do they address the temporal misalignment between transient acoustic events and the chunked, open-loop execution of modern VLA policies.

At the level of physical interaction, a substantial body of work leverages audio as a direct feedback mechanism. Early interactive perception studies demonstrated that robots could estimate material properties based on acoustic responses (Sinapov et al. 2009, 2014). Building on this, recent efforts have utilized sound to assess the stability and gentleness of robotic grasps (Nakahara and Calandra 2025). To scale these capabilities, the community is rapidly moving toward multisensory foundation models. Works such as Audio-VLA explicitly add contact audio perception to large policies, while frameworks like OmniVLA and MLA unify diverse modalities (including vision, language, touch, and audio) into shared representation spaces (Wei et al. 2025; Guo et al. 2025; Liu et al. 2025). Other research has successfully fused contact microphones with vision, demonstrating that audio can serve as a scalable proxy for tactile sensing (Li et al. 2022; Mejia et al. 2024). Complementary to passive listening, active acoustic sensing injects known signals to infer contact states from the acoustic response (Lu and Culbertson 2023; Wall et al. 2023) or uses active excitation through the gripper for long-horizon tasks (Zhang et al. 2025). To process this sensory data, existing methods often plot short audio clips into two-dimensional waveform images, effectively treating sound as an additional static picture, or they rely on fixed-length observation windows strictly aligned with the camera frame rate.

While these models represent a massive leap forward in multimodal representation learning, they face structural challenges when deployed in continuous, real-time control loops. Processing static audio clips or text transcripts works well for identifying loud events or receiving

initial instructions. However, it does not naturally support continuous listening during execution. This structural challenge is exacerbated by the modern control paradigm itself. Because large robot policies often execute actions in open-loop chunks to maintain smooth motion, they create temporary gaps in perception. If a brief acoustic event, such as a microwave “ding”, occurs and finishes outside a predefined observation window or during an execution gap, a static representation cannot capture it.

Scaling auditory capabilities often involves leveraging large-scale pre-trained audio representations, such as CLAP (Elizalde et al. 2023), ImageBind (Girdhar et al. 2023), and BEATs (Chen et al. 2023), which have been successfully fine-tuned within generalist robot policies like FuSe (Jones et al. 2025). However, these foundation models are generally designed to process fixed-length audio clips offline and independently. When deployed in a real-time robotic system, they operate statelessly. This means they do not inherently maintain a temporal context from one clip to the next. Adapting powerful semantic foundation models to operate causally across these discrete control steps remains difficult. Rather than attempting to process a literal continuous analog stream, a primary motivation of our work is to build a general paradigm that maintains temporal context from one clip to the next. By establishing a causal memory across discrete audio windows, we ensure that transient acoustic signals occurring between policy queries are preserved and systematically synchronized with the robot’s control loop.

### 2.3 Datasets and Benchmarks

The recent scaling success of VLA policies is largely driven by massive, standardized datasets. Collaborative efforts like the Open X-Embodiment dataset (O’Neill et al. 2024) have provided millions of visual-kinematic trajectories, enabling models to learn robust generalist behaviors. However, the vast majority of these large-scale resources completely omit the audio modality during data collection. While several pioneering works have recognized this gap and introduced audio-rich manipulation datasets, they typically rely on custom hardware setups. For instance, projects like Play it by Ear (Du et al. 2022) and Hearing Touch (Mejia et al. 2024) collect synchronized audio-visual demonstrations using specialized ear-in-hand microphones or contact sensors during human teleoperation. Although these datasets are highly valuable for proving the utility of acoustic feedback, scaling them to the level required for foundation models presents a significant logistical challenge. Collecting clean, synchronized audio in the real world is highly susceptible to background noise and hardware variability, making it

difficult to aggregate data across different laboratories. To bridge this scaling gap without requiring thousands of hours of new physical data collection, we introduce OpenX-Sound. Rather than recording new real-world audio, our approach leverages advancements in video-to-audio generation models (Luo et al. 2023; Liu et al. 2024a) to retrospectively synthesize temporally aligned acoustic tracks for existing large-scale manipulation episodes. This strategy aligns with recent findings indicating that generative audio can effectively support the learning of multimodal sim-to-real robot policies (Wang et al. 2025a), providing a scalable pathway to pretrain audio-reactive behaviors.

Beyond training data, the field faces a fundamental bottleneck in evaluation infrastructure. Most standard robotic manipulation benchmarks, such as RL Bench (James et al. 2020) and ManiSkill (Gu et al. 2023), are meticulously designed to test spatial reasoning and visual control in silent environments. Simulation platforms that do incorporate acoustics, such as SoundSpaces (Chen et al. 2020), are primarily tailored for mobile navigation toward continuous sound sources rather than reactive manipulation. To address this critical infrastructure gap, we engineered a real-time audio-physics co-simulation platform to establish HEAR-Bench. Unlike standard visual benchmarks, HEAR-Bench natively streams environmental and interaction sounds during physical simulation. Furthermore, it enforces causally strict success rules that actively reject premature actions. This ensures that policies are evaluated on their genuine ability to listen and react to transient sounds in real time.

## 3 The VSLA Paradigm

We formalize the Vision-Sound-Language-Action (VSLA) paradigm. Standard Vision-Language-Action (VLA) implementations predominantly rely on visual and proprioceptive observations to infer environmental states. In contrast, the VSLA paradigm focuses on sound-centric manipulation tasks, where critical physical states or event timings are actively conveyed through acoustic cues. In these scenarios, integrating continuous audio is essential, as sound provides low-level physical feedback and precise success verification that cameras and joint encoders alone cannot capture.

The core theoretical challenge in VSLA is bridging the fundamental temporal mismatch between the continuous, high-frequency nature of acoustic events and the delayed, discrete update cycles of modern robotic policies. To systematically address this, the following subsections define the VSLA observation interface, model the structural blind

spots induced by chunked execution, and formalize the timing-sensitive success criteria required for evaluation.

### 3.1 VSLA Observation and Action Space

**3.1.1 Environment and Signals** We consider a dynamical system evolving in continuous physical time  $\tau \in \mathbb{R}_{\geq 0}$ . The robot runs a low-level controller at frequency  $f_c$  Hz, which induces discrete control cycles indexed by  $t \in \mathbb{N}$ . The physical time corresponding to cycle  $t$  is  $\tau_t \triangleq t/f_c$ .

At each control cycle  $t$ , the robot may receive observations from multiple modalities:

- **Vision** Multi-view RGB images  $I_t^{1:V} = \{I_t^{(1)}, \dots, I_t^{(V)}\}$ .
- **Proprioception** The robot kinematic state  $s_t \in \mathbb{R}^{d_{\text{qpos}}}$ , consisting of joint positions and gripper degree(s) of freedom.
- **Instruction** A natural-language instruction  $l$ , fixed within an episode.
- **Streaming audio** A microphone samples a continuous waveform at rate  $f_s$  Hz. Let  $\mathcal{A}_n \in \mathbb{R}$  denote the  $n$ -th audio sample.

To connect continuous-time audio to discrete control cycles, define the most recent audio sample index available at physical time  $\tau$  as  $n(\tau) \triangleq \lfloor f_s \tau \rfloor$ . At control cycle  $t$ , the most recent available sample index is

$$n_t \triangleq n(\tau_t) = \left\lfloor t \cdot \frac{f_s}{f_c} \right\rfloor. \quad (1)$$

We denote the audio history up to cycle  $t$  as  $\mathcal{H}_t^{\text{audio}} \triangleq (\mathcal{A}_0, \dots, \mathcal{A}_{n_t})$ .

**3.1.2 Observation Interface** The policy is queried only at a subset of control cycles, denoted by decision times  $\{t_k\}_{k \geq 0}$ . Real systems also exhibit non-zero end-to-end latency. We model this latency as an observation delay of  $\tau_{\text{sys}}$  control cycles, meaning that at decision time  $t_k$  the freshest sensor data corresponds to the delayed index

$$\bar{t}_k \triangleq t_k - \tau_{\text{sys}}. \quad (2)$$

We treat  $\tau_{\text{sys}}$  as an integer number of control cycles. If  $t_k < \tau_{\text{sys}}$ , we clip  $\bar{t}_k$  to 0.

For audio, the interface provides a short, causal segment rather than the entire past waveform. Intuitively, at decision time  $t_k$  the policy receives the most recent  $T_{\text{win}}$  seconds of audio that have arrived by the delayed time  $\bar{t}_k$ . Let  $N_{\text{win}} \triangleq \lfloor f_s T_{\text{win}} \rfloor$ . The window is defined as the last  $N_{\text{win}}$  samples up

to index  $n_{\bar{t}_k}$ , padded with zeros when the episode starts:

$$A_{t_k}[i] \triangleq \begin{cases} \mathcal{A}_{n_{\bar{t}_k} - N_{\text{win}} + 1 + i}, & n_{\bar{t}_k} - N_{\text{win}} + 1 + i \geq 0, \\ 0, & \text{otherwise,} \end{cases} \quad (3)$$

for  $i = 0, \dots, N_{\text{win}} - 1$ .

The per-decision VSLA observation is then

$$o_{t_k} \triangleq (I_{\bar{t}_k}^{1:V}, A_{t_k}, l, s_{\bar{t}_k}). \quad (4)$$

This interface makes the delayed decision loop explicit while keeping the audio stream causal.

**3.1.3 Action Space** The robot is controlled by a command vector  $a_t \in \mathbb{R}^{d_{\text{qpos}}}$ , where  $d_{\text{qpos}}$  is the embodiment-specific joint-position dimension including gripper degree(s) of freedom. A low-level controller tracks these commands to drive the physical system.

## 3.2 Temporal Mismatch and the Blind Execution Interval

**3.2.1 Persistence Mismatch Between Vision and Sound** A fundamental distinction between vision and sound in typical manipulation tasks is their behavior under temporal delay. Visual observations primarily encode spatial geometry. Because physical objects possess inertia and robots operate under kinematic constraints, visual states change continuously and remain informative across multiple control cycles. If a camera drops a frame, the object's state can often be reliably interpolated.

In contrast, decision-critical acoustic cues are essentially discrete physical events. They represent abrupt energy releases, such as an impact click or an electronic beep, making them highly transient and non-repeatable. The steady-state audio between these events typically contains low-information ambient noise. When the decision loop is delayed or operates at a low rate, these high-density transient cues may easily fall between observation windows. Unlike visual states, missing an acoustic impulse means the primary evidence of a state transition is permanently lost to the policy.

**3.2.2 Decision Cadence and Latency** Let  $\{t_k\}_{k \geq 0}$  denote the control cycles at which the policy is queried. We define the decision interval and an effective perception-action gap, measured in control cycles, as

$$\Delta_k \triangleq t_{k+1} - t_k, \quad \tau_{\text{sys}} \geq 0, \quad G_k \triangleq \Delta_k + \tau_{\text{sys}}. \quad (5)$$

Here  $\Delta_k$  captures the update cadence of the policy and  $\tau_{\text{sys}}$  aggregates sensing, preprocessing, communication, inference, and actuation delays. The quantity  $G_k$  summarizes how long a transient event may need to persist in order to influence the next decision when only windowed observations are available.

### 3.2.3 Action Chunking and the Blind Execution Interval

Because large backbones are often queried at a rate below the low-level controller, modern systems frequently use action chunking. Let  $t_k$  denote the control cycle at which the  $k$ -th inference is triggered. We denote an action chunk of length  $H$  by

$$\mathbf{a}_k \triangleq (a_{t_k}, a_{t_k+1}, \dots, a_{t_k+H-1}). \quad (6)$$

At each decision, the policy predicts a chunk  $\hat{\mathbf{a}}_k$  that is executed open-loop (Zhao et al. 2023). We denote the executed horizon by  $H_{\text{exec}}$  control cycles, so the next query occurs at  $t_{k+1} = t_k + H_{\text{exec}}$ , which implies  $\Delta_k = H_{\text{exec}}$ . In the common case,  $H_{\text{exec}} = H$  and the entire chunk is executed.

During the interval  $(t_k, t_{k+1})$ , new observations cannot affect the commands currently being executed. We refer to this execution gap as the *Blind Execution Interval* (BEI).

### 3.2.4 Sound Causality and Evidence Vanishing

Transient sound combined with non-zero latency  $\tau_{\text{sys}}$  and delayed or low-rate updates creates an important limitation in sound-centric manipulation. A brief cue can occur and end while the system is executing an open-loop chunk. If the next decision only receives a finite window of recent samples, the cue may no longer appear in the policy input.

To make this concrete, consider the audio-sample indices used to form the next observation. Let a critical event occupy a contiguous sample interval  $[n_e, n_e + D_e)$  in the microphone stream, where  $n_e$  is the start sample index and  $D_e$  is the duration in samples. At decision time  $t_{k+1}$ , the policy forms its audio input from the last  $N_{\text{win}}$  samples available at the delayed time  $\bar{t}_{k+1}$ . This window covers the index interval  $[n_{\bar{t}_{k+1}} - N_{\text{win}} + 1, n_{\bar{t}_{k+1}} + 1)$ .

If the event ends before this window begins, then none of the event samples appear in the next input window:

$$\begin{aligned} n_e + D_e \leq n_{\bar{t}_{k+1}} - N_{\text{win}} + 1 &\implies \\ [n_e, n_e + D_e) \cap [n_{\bar{t}_{k+1}} - N_{\text{win}} + 1, n_{\bar{t}_{k+1}} + 1) &= \emptyset. \end{aligned} \quad (7)$$

In other words, the acoustic event terminates strictly before the new observation window begins. In this case, a window-only interface provides no direct evidence that the event occurred. This motivates the necessity of maintaining a

causal memory state that persists across decision gaps so that short acoustic cues occurring during  $(t_{k-1}, t_k)$  remain available at the next decision.

Concretely, we require a causal state update function  $f_\varphi$  and a chunk policy  $\pi_\theta$  such that:

$$\begin{aligned} h_{t_k} &= f_\varphi(h_{t_{k-1}}, \mathcal{A}_{n_{\bar{t}_{k-1}}+1:n_{\bar{t}_k}}), \\ \hat{\mathbf{a}}_k &= \pi_\theta(o_{t_k}, h_{t_k}). \end{aligned} \quad (8)$$

This requirement captures the need for sound-centric manipulation under delayed, chunked execution. Transient cues that occur during an execution gap must be summarized into  $h_{t_k}$  so they can inform the next decision.

## 3.3 Temporal Grounding and Motion Collapse

Capturing a transient cue is necessary but not sufficient. Sound-centric tasks often include long monitoring phases in which the robot must hold a stable posture and wait, followed by a rapid reaction once an acoustic trigger occurs. During such phases, the visual scene can be quasi-static and provides weak information about temporal progression. Under these conditions, successive observations can be nearly indistinguishable for many decisions, even though the desired control behavior changes over time.

This creates temporal aliasing that is common in partially observable settings (Heess et al. 2015). There may exist two decision indices  $k \neq k'$  such that the available observations are similar while the expert action chunks differ:

$$o_{t_k} \approx o_{t_{k'}} \quad \text{but} \quad \mathbf{a}_k^* \neq \mathbf{a}_{k'}^*. \quad (9)$$

In intuitive terms, the robot experiences a “waiting dilemma”: it sees the same static scene frame after frame, making it difficult to maintain a steady posture without an internal sense of elapsing time. In practice, this mismatch can lead to unstable waiting behavior under chunked execution, including drift or freezing. It relates closely to the Temporal Motion Collapse phenomenon reported for long-horizon chunked policies (Zhao et al. 2023).

A practical way to mitigate this issue is to encourage the policy representation to encode the flow of time even when vision changes little. Audio is well-suited for this role because it evolves continuously and often reflects ongoing physical processes. In our setting, this motivates auxiliary predictive objectives that use near-future audio as supervision, so that the latent representation learns to anticipate how the soundscape will evolve. This provides temporal grounding without introducing additional evaluation criteria, and it matches the constraints

of streaming, causal deployment (Jaderberg et al. 2017; Arandjelovic and Zisserman 2017).

### 3.4 Learning Objective and Causal Evaluation

**3.4.1 Timed Success Criteria** Sound-centric manipulation is timing-sensitive. Reaching the geometric goal before the relevant acoustic cue should be counted as failure, even if the final state looks visually correct.

Let  $g(\mathcal{H}_t^{\text{audio}}) \in \{0, 1\}$  be a task-specific predicate that becomes true when the cue condition is satisfied, for example when a beep starts. Define  $t_{\text{snd}} = \min\{t \in \{0, \dots, T\} : g(\mathcal{H}_t^{\text{audio}}) = 1\}$ . Let  $x_t$  denote the environment state used to evaluate task completion, for example privileged simulator state in benchmark settings. Let  $T$  denote the maximum discrete length of the episode. Define  $t_{\text{goal}} = \min\{t \in \{0, \dots, T\} : \text{Goal}(x_t) = 1\}$ , with the convention  $\min \emptyset = +\infty$ . We evaluate a trajectory  $\xi$  using the timing-sensitive success indicator

$$\text{Success}(\xi) = \mathbb{1}[t_{\text{snd}} \leq t_{\text{goal}} \leq T]. \quad (10)$$

This rule enforces sound causality at evaluation time by rejecting early actions that reach the goal before the cue and by treating trajectories without a cue event as failure.

**3.4.2 Learning Objective** We adopt imitation learning from expert demonstrations. At each decision time  $t_k$ , the expert executes an action chunk of length  $H$ ,

$$\mathbf{a}_k^* \triangleq (a_{t_k}^*, \dots, a_{t_k+H-1}^*), \quad (11)$$

and the learner predicts a chunk  $\hat{\mathbf{a}}_k$  conditioned on the available observation  $o_{t_k}$  and a causal memory  $h_{t_k}$ .

At the formulation level, we treat the learner as a conditional action-chunk model trained to match expert behavior under the VSLA interface and its causal constraints. The concrete instantiation can be a deterministic regressor or a conditional generative model, and it may include auxiliary objectives to encourage causal persistence and temporal grounding. The specific training losses used in our approach are described in Section 4.

## 4 The HEAR Framework

While the VSLA paradigm establishes the theoretical constraints for sound-centric control, realizing it on physical hardware requires a specific architecture. We present HEAR, an end-to-end framework that instantiates the VSLA paradigm under delayed, low-rate, and asynchronous decision loops. As formalized in Section 3, sound-centric

manipulation highlights two timing-related difficulties. First, short-lived acoustic cues can occur within the effective perception-action gap and may leave the fixed audio window before the next decision, providing no evidence in a window-only interface (Eq.(7)). This issue is especially pronounced under open-loop action chunking, where the Blind Execution Interval suppresses perception updates during execution. Second, many sound-centric tasks involve extended monitoring phases with quasi-static vision. In such phases, snapshot observations can be nearly indistinguishable across decisions (Eq.(9)), and chunked control can become unstable over long horizons consistent with Temporal Motion Collapse (Zhao et al. 2023).

HEAR follows a simple systems view to resolve these bottlenecks. Since large backbones cannot be queried at sensor rates in real robots, we decouple high-frequency auditory sensing from low-frequency reasoning and action generation. A lightweight audio buffer is maintained to continuously record transient acoustic events between policy queries. The main policy then operates at a slower control rate, conditioning its decisions on the contents of this buffer. In addition, we introduce a predictive learning signal on near-future audio dynamics, which encourages the shared representation to encode the flow of time even when vision changes little.

HEAR comprises four modules in the following order. The **Historizer** maintains a causal audio memory that bridges execution gaps (Section 4.2). The **Envisioner** fuses multi-modal inputs into compact representations for control (Section 4.3). The **Advancer** predicts near-future audio codes from the Envisioner latent to provide temporal grounding during learning (Section 4.4). The **Realizer** then generates smooth action chunks for continuous control (Section 4.5). Figure 2 illustrates the overall data flow.

### 4.1 Architectural Overview

We follow the VSLA observation interface in Eq. (4). At decision time  $t_k$ , the freshest sensor data corresponds to the delayed index  $\bar{t}_k$  (Eq. (2)), and the per-decision observation is  $o_{t_k} = (I_{\bar{t}_k}^{1:V}, A_{t_k}, l, s_{\bar{t}_k})$ . The audio window  $A_{t_k}$  contains only the most recent  $T_{\text{win}}$  seconds of waveform available by  $\bar{t}_k$  (Eq. (3)). When a cue is brief and the next decision is delayed, the cue can fall outside this window and become unavailable at the next query (Eq. (7)).

HEAR augments this interface with a persistent audio memory  $h_{t_k}$  computed from streaming audio arriving between delayed boundaries  $\bar{t}_{k-1}$  and  $\bar{t}_k$ . The Historizer updates this memory independently of the policy query cadence. The Envisioner then maps the observation together

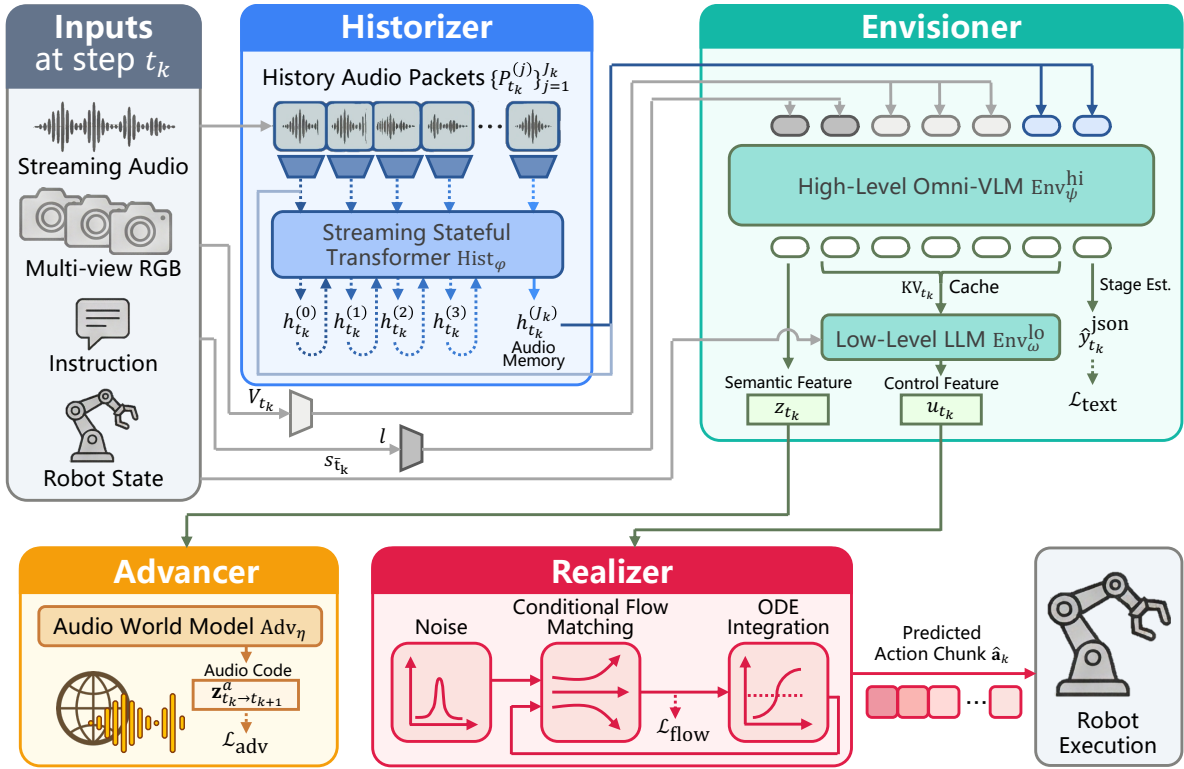


**Figure 2. The HEAR framework architecture.** The **Historizer** processes audio packets with a Streaming Stateful Transformer that maintains a compact causal memory  $h_{t_k}$  and bridges execution gaps, including the Blind Execution Interval induced by open-loop chunking. The **Envisioner** employs a hierarchical design. Its high-level omni-modal model integrates multimodal inputs, including vision, instruction, robot state, and audio context, and outputs a semantic latent  $z_{t_k}$  and a key–value cache  $KV_{t_k}$ . It also predicts a text stage description  $\hat{y}_{t_k}^{\text{json}}$ . Its low-level model reuses  $KV_{t_k}$  together with the current state and extracts a control feature  $u_{t_k}$ . The **Advancer** is a decoder-only transformer that predicts a near-future audio code sequence  $\mathbf{z}_{t_k \rightarrow t_{k+1}}^a$  from  $z_{t_k}$  during training. The **Realizer** synthesizes smooth action chunks via Conditional Flow Matching conditioned on  $u_{t_k}$ .

with  $h_{t_k}$  into a semantic latent  $z_{t_k}$  and a low-dimensional control embedding  $u_{t_k}$ . During learning, the Advancer predicts near-future audio codes from  $z_{t_k}$ , which encourages the shared representation to reflect temporal progression under quasi-static vision. Finally, the Realizer generates an  $H$ -step action chunk from  $u_{t_k}$  that is executed open-loop.

We summarize the computation at decision time  $t_k$  as:

$$\begin{aligned} h_{t_k} &= f_\varphi(h_{t_{k-1}}, \mathcal{A}_{n_{\bar{t}_{k-1}}+1:n_{\bar{t}_k}}), \\ (z_{t_k}, u_{t_k}) &= g_\psi(o_{t_k}, h_{t_k}), \\ p_\eta(\mathbf{z}_{t_k \rightarrow t_{k+1}}^a | z_{t_k}) &= \text{Adv}_\eta(z_{t_k}), \\ \hat{\mathbf{a}}_k &\sim \pi_\theta(\cdot | u_{t_k}). \end{aligned} \quad (12)$$

Here,  $f_\varphi$  denotes the streaming audio update,  $g_\psi$  denotes the Envisioner encoder,  $\text{Adv}_\eta$  denotes the Advancer network parameterized by  $\eta$ , and  $\pi_\theta$  denotes the action-chunk generator. The predicted chunk  $\hat{\mathbf{a}}_k = (\hat{a}_{t_k}, \dots, \hat{a}_{t_k+H-1})$  is executed open-loop for  $H_{\text{exec}}$  control cycles (Section 3.2.3). The Advancer branch provides a predictive learning signal that shapes the latent representation  $z_{t_k}$ . At deployment, HEAR does not need to explicitly generate the future audio

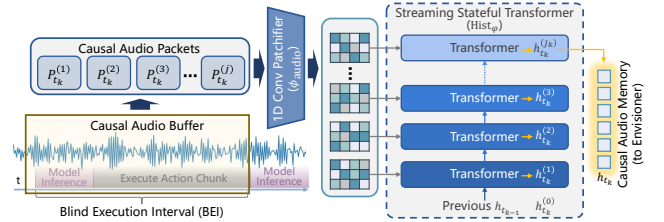


**Figure 3. The Historizer module.** It processes continuous audio streams into discrete packets and uses a streaming stateful transformer to maintain a persistent causal memory. This mechanism ensures that transient acoustic events occurring during blind execution intervals are preserved for the next decision cycle.

codes  $\mathbf{z}_{t_k \rightarrow t_{k+1}}^a$ , but the temporal structure induced by this objective remains in the latent and benefits control.

## 4.2 Historizer

As shown in Figure 3, the Historizer provides causal persistence for transient acoustic cues. In sound-centric manipulation, a brief event can occur while the robot is executing an open-loop action chunk, yet it may not appear in the next fixed audio window  $A_{t_{k+1}}$ . To keep such evidence available for the next decision, the Historizer maintains a

compact memory state that is updated from streaming audio independently of the policy query cadence.

**4.2.1 Streaming Stateful Summarization** We distinguish the fixed per-decision window  $A_{t_k}$  (Eq. (3)) from the streaming packets used by the Historizer. At decision time  $t_k$ , due to end-to-end latency, the freshest audio available to the system corresponds to the delayed boundary  $\bar{t}_k$  (Eq. (2)). We therefore update the memory using the newly arrived samples between successive delayed boundaries,  $\mathcal{A}_{n_{\bar{t}_{k-1}}+1:n_{\bar{t}_k}}$ . We partition this stream into  $J_k$  short causal packets  $\{P_{t_k}^{(j)}\}_{j=1}^{J_k}$  ordered from old to new, where each packet contains  $L$  samples. In practice, these packets can be accumulated in a small ring buffer and processed online as they arrive, while we simply read out the current memory at decision times.

We implement the Historizer as a Streaming Stateful Transformer that carries a compact memory across packets. A lightweight causal audio frontend  $\phi_{\text{audio}}$  maps each packet to token features, using a small causal 1D convolutional patchifier. The memory update is

$$\begin{aligned} h_{t_k}^{(0)} &= h_{t_{k-1}}, \\ h_{t_k}^{(j)} &= \text{Hist}_\varphi\left(h_{t_k}^{(j-1)}, \phi_{\text{audio}}(P_{t_k}^{(j)})\right), \quad j = 1, \dots, J_k, \\ h_{t_k} &= h_{t_k}^{(J_k)}, \end{aligned} \quad (13)$$

where  $\text{Hist}_\varphi$  denotes the core transformer block parameterized by  $\varphi$ , and  $h_{t_k}$  is the final causal audio memory provided to the Envisioner at decision time  $t_k$ . At the beginning of an episode ( $k = 0$ ), the initial memory  $h_{t_{-1}}$  is set to a zero vector. This streaming process instantiates the general update function  $f_\varphi$  defined in Eq. (12). This update is causal because it depends only on audio that has arrived by  $\bar{t}_k$ .

**4.2.2 Bridging Execution Gaps** Because  $\{P_{t_k}^{(j)}\}$  covers the audio that arrives between delayed decision boundaries, short-lived cues that occur during open-loop execution can still be incorporated into  $h_{t_k}$ . This reduces the chance of evidence vanishing (Eq. (7)) by ensuring that the next decision can condition on a persistent summary of what happened acoustically since the previous query.

A practical requirement is that the Historizer has sufficient effective coverage horizon  $T_{\text{mem}}$ , so that salient evidence remains representable in  $h_{t_k}$  until the next decision that needs it. A useful design target is

$$T_{\text{mem}} \geq \frac{\max_k \Delta_k + \tau_{\text{sys}}}{f_c}, \quad (14)$$

so that a transient cue occurring within the effective perception-action gap can still influence the next decision.

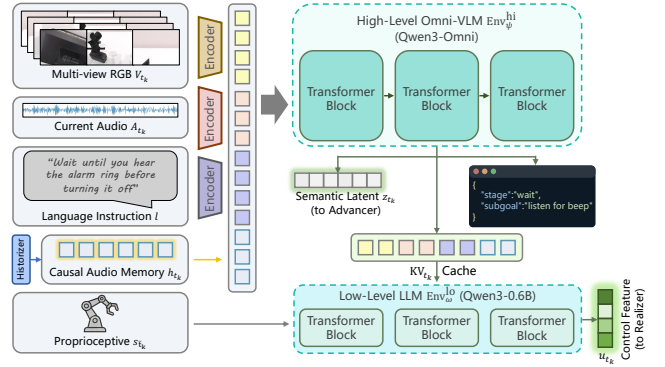


**Figure 4. The Envisioner module.** A hierarchical reasoning architecture fuses multimodal inputs to guide manipulation. The high-level omni-modal model extracts semantic latents and stage descriptions, while the low-level model reuses the resulting key-value cache alongside proprioceptive data to efficiently generate control features.

Finally, maintaining a memory state allows us to keep the fixed input window  $A_{t_k}$  relatively modest. In our experience, relying on a very long window alone can mix distinct interaction phases and make performance more sensitive to the exact window length. By combining a short causal window with a persistent summary  $h_{t_k}$ , HEAR can retain relevant history while staying aligned with streaming, delayed deployment.

### 4.3 Envisioner

As depicted in Figure 4, the Envisioner serves as the perception-and-reasoning core of HEAR. It adopts a coarse-to-fine hierarchical architecture, implementing the encoder  $g_\psi$  in Eq. (12). At each decision time  $t_k$ , it fuses the VSLA observation  $o_{t_k}$  with the Historizer memory  $h_{t_k}$ . Its design separates slow multi-modal reasoning from fast control decoding. Concretely, a high-level omni-modal module of Qwen3-Omni (Xu et al. 2025) summarizes the multi-modal context and produces three outputs: (i) a semantic latent  $z_{t_k}$  for temporal learning in the Advancer, (ii) a key-value cache  $KV_{t_k}$  for efficient reuse by a lightweight low-level module of Qwen3-0.6B (Yang et al. 2025), and (iii) a structured stage description  $\hat{y}_{t_k}^{\text{json}}$  generated by the high-level model’s text head. A low-level module then conditions on  $KV_{t_k}$  together with the current robot state to produce a low-dimensional control feature  $u_{t_k}$  for the Realizer.

**4.3.1 High-Level Omni-LLM** We denote the high-level module as  $\text{Env}_\psi^{\text{hi}}$ . Its inputs follow the VSLA interface:

- Multi-view RGB images  $V_{t_k} \triangleq I_{t_k}^{1:V}$ .
- Natural language instruction  $l$ .
- Robot proprioceptive state  $s_{\bar{t}_k}$ .
- The current audio window  $A_{t_k}$  (Eq. (3)).

- The causal audio memory  $h_{t_k}$  from the Historizer.

The module produces a semantic latent  $z_{t_k}$  and a KV cache  $KV_{t_k}$  for reuse:

$$(z_{t_k}, KV_{t_k}) = \text{Env}_{\psi}^{\text{hi}}(V_{t_k}, A_{t_k}, l, s_{\bar{t}_k}, h_{t_k}). \quad (15)$$

In addition, leveraging its native text generation capability, it outputs a structured stage record  $\hat{y}_{t_k}^{\text{json}}$  at the same time.

**4.3.2 Stage Decomposition** Sound-centric tasks often contain visually similar phases with different intent, such as holding still to monitor versus acting after a trigger. To make this progress explicit, the high-level module generates a short structured stage description  $\hat{y}_{t_k}^{\text{json}}$ , for example `{"stage": "wait", "subgoal": "listen for beep"}`. We train this output by minimizing token-level negative log-likelihood over the JSON string. We denote this auxiliary objective as  $\mathcal{L}_{\text{text}}$ . This loss encourages the semantic latent  $z_{t_k}$  to track progress and to separate phases that may be visually quasi-static but acoustically distinct.

**4.3.3 Low-Level LLM** The low-level module  $\text{Env}_{\omega}^{\text{lo}}$  produces a control feature vector  $u_{t_k}$  by reusing the cached context  $KV_{t_k}$  together with the robot state:

$$u_{t_k} = \text{Env}_{\omega}^{\text{lo}}(KV_{t_k}, s_{\bar{t}_k}). \quad (16)$$

This design reuses the high-level multi-modal context while keeping the control pathway lightweight. The resulting  $u_{t_k}$  serves as the conditioning signal for the Realizer, which generates the action chunk executed after time  $t_k$ .

## 4.4 Advancer

Capturing a transient cue is necessary, but long-horizon monitoring also requires a stable notion of time. When vision is quasi-static, a policy that only sees snapshot observations may receive nearly identical inputs across many decisions, even though the desired behavior changes with elapsed time (Eq. (9)). The Advancer addresses this by learning audio dynamics through near-future prediction, as shown in Figure 5. This predictive learning encourages the shared latent  $z_{t_k}$  to reflect temporal progression, which can improve stability during extended listening phases and sharpen reactivity once a cue occurs.

**4.4.1 Near-Future Audio Codes** Rather than predicting raw waveforms, we predict discrete audio codes obtained from a neural audio tokenizer. Let  $\text{Tok}(\cdot)$  map a waveform segment to a sequence of discrete code indices. We use a causal streaming tokenizer so that the codes for a segment

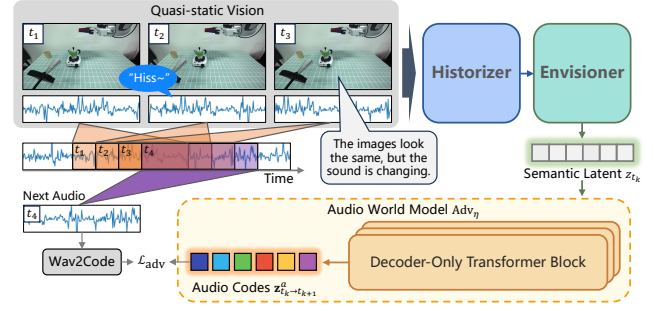


**Figure 5. The Advancer module.** In scenarios requiring sustained waiting with quasi-static visual observations, this decoder-only audio world model predicts near-future acoustic codes. This predictive objective grounds the shared latent representation in continuous time, helping the policy maintain stability and temporal awareness.

depend only on samples within that segment, matching the constraints of streaming deployment (Défossez et al. 2024).

We define the prediction target as the code sequence for the audio that arrives after the delayed boundary  $\bar{t}_k$  and up to the next delayed boundary  $\bar{t}_{k+1}$ :

$$\mathbf{z}_{t_k \rightarrow t_{k+1}}^a \triangleq \text{Tok}(\mathcal{A}_{n_{\bar{t}_k+1}: n_{\bar{t}_{k+1}}}). \quad (17)$$

This definition makes explicit that the target corresponds to a time interval, rather than a single instant. Note that while we denote the target with the decision interval subscript  $t_k \rightarrow t_{k+1}$  for simplicity, the actual prediction interval is strictly aligned with the delayed boundaries  $\bar{t}_k$  and  $\bar{t}_{k+1}$  to respect causality. Because Tok is causal, the codes for this interval depend only on samples within the interval, which is consistent with streaming constraints.

**4.4.2 Latent Prediction** The Advancer, denoted as  $\text{Adv}_{\eta}$ , is implemented as a decoder-only predictor parameterized by  $\eta$  that takes  $z_{t_k}$  as input and outputs a distribution over the future code sequence:

$$p_{\eta}(\mathbf{z}_{t_k \rightarrow t_{k+1}}^a | z_{t_k}) = \text{Adv}_{\eta}(z_{t_k}). \quad (18)$$

We train it with cross-entropy over codebook indices:

$$\mathcal{L}_{\text{adv}} = -\mathbb{E}_{\mathcal{D}} \left[ \log p_{\eta}(\mathbf{z}_{t_k \rightarrow t_{k+1}}^a | z_{t_k}) \right]. \quad (19)$$

where  $\mathcal{D}$  denotes the training dataset. At deployment, HEAR does not need to explicitly generate  $\mathbf{z}_{t_k \rightarrow t_{k+1}}^a$ . The role of the Advancer is to inject a concrete temporal learning signal into the shared latent, so that  $z_{t_k}$  better tracks time-evolving process states when vision changes little.

## 4.5 Realizer

The Realizer maps the low-level control feature  $u_{t_k}$  to an  $H$ -step joint-position action chunk  $\hat{\mathbf{a}}_k = (\hat{a}_{t_k}, \dots, \hat{a}_{t_k+H-1})$ . The robot then executes this chunk open-loop for  $H_{\text{exec}}$  control cycles, as described in Section 3.2.3. We model the Realizer as a conditional generator,

$$\hat{\mathbf{a}}_k \sim \pi_\theta(\cdot | u_{t_k}). \quad (20)$$

In sound-centric manipulation, smooth chunks are useful for tracking accuracy, and they can also make listening more reliable. Abrupt motion may introduce mechanical ego-noise and transient vibration that mask weak acoustic cues, especially during monitoring phases (Liu et al. 2024b).

We instantiate  $\pi_\theta$  using conditional flow matching (CFM) (Lipman et al. 2023; Liu et al. 2023). CFM learns a continuous vector field that transports samples from a simple Gaussian prior to the action-chunk distribution along a straight-line path. This structure is convenient for real robots because it can generate chunks with a small, fixed number of integration steps. Compared with diffusion-style action generators (Chi et al. 2025), this can reduce the inference overhead in low-rate decision loops.

**4.5.1 Conditioning** We condition the flow network on  $u_{t_k}$  using adaptive normalization. Concretely, a small MLP maps  $u_{t_k}$  to per-block scale and shift parameters, and these parameters modulate the normalized activations (Perez et al. 2018). This provides a lightweight way to adapt the generated action distribution to the inferred task context (Lipman et al. 2023).

**4.5.2 Vector Field Regression** Let  $\mathbf{a}_k^*$  be the expert action chunk of length  $H$  at decision time  $t_k$  (Eq. (11)). We flatten the chunk into a vector  $x_1 \triangleq \text{vec}(\mathbf{a}_k^*) \in \mathbb{R}^{Hd_{\text{apos}}}$ , and sample Gaussian noise  $x_0 \sim \mathcal{N}(0, I)$ . For flow time  $\lambda \in [0, 1]$ , we define the linear transport path  $x_\lambda = (1 - \lambda)x_0 + \lambda x_1$ .

The Realizer learns a conditional vector field  $v_\xi(x_\lambda, \lambda, u_{t_k})$  and regresses it to the target direction  $(x_1 - x_0)$ :

$$\mathcal{L}_{\text{flow}} = \mathbb{E}_{x_0 \sim \mathcal{N}(0, I), \lambda \sim \mathcal{U}(0, 1)} \left[ \|v_\xi(x_\lambda, \lambda, u_{t_k}) - (x_1 - x_0)\|_2^2 \right], \quad (21)$$

where  $u_{t_k}$  is produced by the low-level Envisioner from  $(\text{KV}_{t_k}, \text{S}_{t_k})$  (Eq. (16)).

**4.5.3 Inference via Euler Integration** At test time, we sample  $x_0$  and numerically integrate the ODE defined by the learned vector field:

$$\frac{dx_\lambda}{d\lambda} = v_\xi(x_\lambda, \lambda, u_{t_k}), \quad (22)$$

from  $\lambda = 0$  to  $\lambda = 1$ . To satisfy real-time constraints, we use Euler integration with a fixed number of steps. The solution at  $\lambda = 1$  yields  $\hat{x}_1$ , which we reshape into the predicted action chunk  $\hat{\mathbf{a}}_k$  and execute open-loop for  $H_{\text{exec}}$  cycles.

## 4.6 Training Objectives

We train HEAR with imitation learning from expert action chunks. Each training sample contains the per-decision observation  $o_{t_k}$  (Eq. (4)), the expert action chunk  $\mathbf{a}_k^*$  (Eq. (11)), and a stage label  $y_{t_k}^{\text{json}^*}$ . We denote the dataset of extracted training samples as  $\mathcal{D} = \{(o_{t_k}, \mathcal{A}_{n_{\bar{t}_k-1}+1:n_{\bar{t}_k+1}}, \mathbf{a}_k^*, y_{t_k}^{\text{json}^*})\}_{k=1}^N$ , which explicitly includes the continuous audio segments required for the Historizer memory update and the Advancer target.

The total objective is a weighted sum:

$$\mathcal{L}_{\text{total}} = \mathcal{L}_{\text{flow}} + w_{\text{adv}} \mathcal{L}_{\text{adv}} + w_{\text{text}} \mathcal{L}_{\text{text}}, \quad (23)$$

where  $\mathcal{L}_{\text{flow}}$  trains the Realizer for action-chunk generation (Eq. (21)),  $\mathcal{L}_{\text{adv}}$  trains the Advancer for near-future audio code prediction (Eq. (19)), and  $\mathcal{L}_{\text{text}}$  supervises the structured stage description generated by the high-level Envisioner (Section 4.3.2).

In practice, we gradually increase  $w_{\text{adv}}$  and  $w_{\text{text}}$  during early training. This lets the model first learn basic action imitation, and then place more emphasis on temporal grounding and progress tracking.

## 5 Data and Benchmark Suite

Although large-scale VLA datasets and benchmarks have driven significant progress in robot learning, they are fundamentally insufficient for VSLA research. They rarely provide synchronized audio streams for training, nor do they enforce timing-aware, sound-causal rules for evaluation. To overcome these practical bottlenecks, we introduce two supporting resources. The first is OpenX-Sound, an audio-augmented dataset derived from Open X-Embodiment designed to support scalable pretraining with streaming audio. The second is HEAR-Bench, a sound-centric simulation benchmark that standardizes fine-tuning and evaluation under strict sound-causal success criteria (as defined in Section 3.4.1). Together, these tools provide a necessary foundation for training and evaluating policies that must listen, wait, and react in real time.

## 5.1 OpenX-Sound: Audio-Augmented Open X-Embodiment

The original Open X-Embodiment (OpenX) dataset (O’Neill et al. 2024) provides exceptional task coverage and embodiment diversity, yet it lacks microphone recordings entirely. Because collecting synchronized, high-quality audio at such a massive scale is logistically prohibitive and difficult to standardize across different laboratories, we construct OpenX-Sound retrospectively. We select a subset of OpenX episodes suitable for sound-centric manipulation and augment each trajectory with a time-aligned waveform. These waveforms are synthesized directly from the original video tracks using recent video-to-audio generation models (Luo et al. 2023; Liu et al. 2024a). We emphasize that OpenX-Sound is intended exclusively for scalable pretraining, allowing the model to bootstrap streaming-audio representation learning and multimodal grounding before fine-tuning on real physical data.

**Scale and Diversity.** For every selected OpenX episode, we preserve all original signals, including multi-view RGB, language instructions, proprioception, and expert actions, while attaching the newly synthesized audio track. As summarized in Table 1, OpenX-Sound inherits the broad diversity of its source material. The interaction patterns are equally diverse, encompassing simple pick-and-place actions, complex tool use, articulated-object manipulation.

**Table 1. Key statistics of OpenX-Sound.** This selected subset of Open X-Embodiment episodes is augmented with synchronized audio tracks to support large-scale VSLA pretraining.

Statistic	Value
Episodes	~120k
Skills	100
Robot mass range	~7–120 kg
Modalities	RGB, language, qpos, actions, <b>audio</b>
Audio format	waveform, $f_s=16$ kHz

**Audio Synthesis and Alignment.** During the dataset construction, modern video-to-audio models produce perceptually plausible acoustic tracks that include both ambient background noise and explicit interaction sounds (e.g., machine hums, impact clicks). This provides a rich source of acoustic variation. At training time, OpenX-Sound adheres strictly to the streaming interface defined in our formulation. At any decision time  $t_k$ , the policy receives a causal audio window  $A_{t_k}$  (Eq. (3)). This ensures that the pretraining phase remains structurally consistent with delayed, windowed deployment on physical hardware.

**Dataset Validation.** Because downstream VSLA tasks are highly sensitive to timing, we conducted a manual audit to verify that the generated audio is both temporally synchronized with the video and semantically relevant to the physical manipulation. We randomly sampled 500 episodes and assigned two annotators to each. The audit revealed a 98.7% synchronization accuracy within a 100 ms tolerance. These results indicate that OpenX-Sound provides reliable temporal and semantic grounding for pretraining purposes.

Given the domain gap between synthesized and physical acoustics (e.g., unmodeled room impulse responses, variable microphone placements, mechanical ego-noise), OpenX-Sound serves strictly for pretraining. Unless specified, all simulation and real-robot evaluations in Section 6 fine-tune an OpenX-Sound checkpoint on task-specific real-audio demonstrations.

## 5.2 HEAR-Bench: Sound-Centric Simulation Benchmark

While large datasets facilitate representation learning, standard manipulation benchmarks (e.g., RL-Bench (James et al. 2020), ManiSkill (Gu et al. 2023)) typically operate in silent environments and cannot evaluate auditory reactivity. To address this, we introduce HEAR-Bench, a sound-enabled manipulation benchmark built upon the RoboTwin2 platform (Chen et al. 2025) (shown in Figure 6(a)). HEAR-Bench features a streaming microphone channel and enforces strict sound-causal success rules.

**Simulation platform and audio pipeline.** To make the simulator audible and support online recording, we implemented a dedicated audio thread that runs asynchronously alongside the physics engine. By default, this thread emits ambient environmental noise. When task-defined trigger conditions occur, such as a randomized alarm or a physical contact event, the simulator injects the corresponding audio clip into the background stream to simulate in-environment playback. At each control cycle, the environment reads the most recent samples from this stream to form the causal window  $A_{t_k}$ . We align the injected clip onset to the audio stream at the exact sample index computed by Eq. (1), ensuring that the timing between the physics steps and the waveform buffer remains deterministic.

**A Taxonomy of Manipulation Sounds.** To systematically evaluate auditory awareness, we organize the decision-critical acoustic cues in HEAR-Bench into four primary categories derived from everyday human experience: human speech, event-triggered alarms, continuous process sounds,

and physical interaction feedback. We instantiate these categories across seven distinct tasks, as detailed in Table 2.

**Table 2. HEAR-Bench tasks.** The benchmark evaluates four primary categories of decision-critical acoustic cues under strict temporal constraints.

Task	Primary cue
<b>Event-triggered alarms</b>	
<i>Alarm Clock</i>	alarm ringing
<i>Microwave</i>	completion beep
<b>Human speech</b>	
<i>Check Yes</i>	prosody-driven speech
<i>Interrupt</i>	spoken interruption
<b>Continuous process sounds</b>	
<i>Pour Water</i>	pouring sound evolution
<i>Boil Water</i>	boiling sound evolution
<b>Physical interaction feedback</b>	
<i>Check Materials</i>	contact acoustics

- *Alarm Clock* and *Microwave* require reacting to event-triggered alarms. These tasks test whether the policy can wait and then act *after* the cue.
- *Check Yes* and *Interrupt* require understanding speech beyond transcript-level content, including prosody and timing.
- *Pour Water* and *Boil Water* require continuous process monitoring, where sound evolves while vision can be weak or quasi-static.
- *Check Materials* requires using physical interaction feedback to infer material properties under visually ambiguous conditions.

**Embodiment and Arm Selection.** Because RoboTwin2 is dual-arm (Figure 6(a)), HEAR-Bench exposes joint-position control for both arms. For tasks with a single interaction target, the policy must also resolve which arm should act. In particular, *Alarm Clock* and *Interrupt* require the model to choose whether the left or right arm executes the press or reset behavior while keeping the other arm stable.

**Sound-Causal Evaluation Protocol.** The characteristic of HEAR-Bench is its timing-sensitive evaluation. Across all tasks, success is strictly governed by Eq. (10). If the robot reaches the geometric goal before the relevant acoustic cue has occurred, the trial is recorded as a failure. We randomize initial visual states and cue timings to prevent policies from memorizing visual sequences or exploiting spurious correlations. By combining short-lived cues and long waiting phases, HEAR-Bench can directly test whether a policy can successfully bridge sensory execution gaps in real time.

## 6 Experiments

We evaluate HEAR in two distinct settings to demonstrate the versatility of the VSLA paradigm across different robot architectures and acoustic environments. The first setting is a sound-enabled simulation on HEAR-Bench (Section 5.2), utilizing the dual-arm RoboTwin2 platform (Figure 6a). The second involves real-world deployment on a single-arm Franka Panda (Figure 6b). In both environments, acoustic cues are critical for decision-making. Importantly, a trial is considered successful only if the robot completes the physical goal strictly after the relevant sound condition is satisfied, adhering to the causal success criteria defined in Section 3.4.1. We report this success rate as our primary evaluation metric.

Our experimental design is structured to address three core research questions. First, can a policy reliably utilize diverse acoustic cues—ranging from transient impacts to continuous process sounds and nuanced speech prosody—for closed-loop manipulation? Second, can the system gracefully handle cue dropout under delayed or low-rate decision loops? This is particularly challenging when fleeting acoustic evidence falls outside a short observation window or occurs during an open-loop execution gap. Finally, how do the individual architectural components of HEAR contribute to mitigating specific sound-centric failure modes?

To address these questions rigorously, we specifically designed our tasks to isolate the necessity of acoustic information. In these scenarios, a policy relying solely on vision might generate movements that appear correct, but it will ultimately fail under our sound-based success criteria in Eq. (10). We enforce this reliance through long waiting phases, visually ambiguous states, and continuous processes where the critical progress variable is encoded exclusively in the temporal evolution of sound.

### 6.1 Experimental Setup

**6.1.1 Observation Interface and Action Space** All evaluated methods operate strictly under the formal VSLA observation interface defined in Eq. (4). At decision time  $t_k$ , the policy receives multi-view RGB images  $I_{t_k}^{1:V}$ , a causal audio window  $A_{t_k}$ , a natural language instruction  $l$ , and proprioception  $s_{\bar{t}_k}$ . The audio input is consistently provided as a 1D raw waveform vector sampled from a single microphone, ensuring the external interface remains uniform even if specific baselines compute spectrograms internally. Proprioception consists of the robot’s joint-position state (qpos), encompassing all controllable joints and gripper degrees of freedom. At each inference step  $t_k$ , the policy

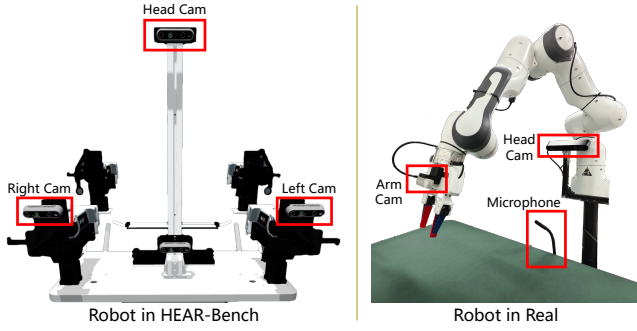


**Figure 6. Robot platforms and sensor suites.** (a) For HEAR-Bench simulations, we use a dual-arm RoboTwin2 equipped with three RGB camera views (Head Cam, Left Cam, Right Cam). (b) For real-world experiments, we deploy a single-arm Franka Panda with a head-mounted camera, an arm-mounted camera, and a standard workspace microphone.

generates an action chunk of joint-position targets  $\hat{\mathbf{a}}_k \in \mathbb{R}^{H \times d_{\text{qpos}}}$ . To ensure a controlled comparison, we maintain a consistent chunk horizon of  $H = 32$  across all methods unless explicitly stated otherwise.

Following the minimalist design of recent end-to-end systems (Intelligence et al. 2025), our control pipeline is highly simplified. The predicted action chunks encode target joint and gripper positions, which are unrolled and executed open-loop at 30 Hz ( $f_c = 30$  Hz). These targets are directly tracked by a simple low-level PD controller, without relying on any additional trajectory planning, inverse kinematics solvers, or collision detection.

We evaluate two distinct robot configurations (Figure 6). In the HEAR-Bench simulation, we utilize the dual-arm RoboTwin2 platform equipped with three RGB camera views (head, left, and right). For real-world deployments, we use a single-arm Franka Panda equipped with a head-mounted RGB camera, an arm-mounted RGB camera, and a standard workspace microphone.

**6.1.2 Training Protocol and Implementation Details** All policies are trained via offline imitation learning using a two-stage recipe: an initial pretraining phase on the OpenX-Sound dataset (Section 5.1) to establish foundational multi-sensory representations, followed by task-specific fine-tuning on either HEAR-Bench or real-robot demonstrations. We evaluate each task over 100 independent trials, randomizing initial visual scenes and cue timings to prevent policies from memorizing fixed temporal schedules.

The **Historizer** employs a Streaming Stateful Transformer that processes audio packets sequentially ( $L = 640$  samples, or 40 ms per packet), maintaining a compact memory of 16 tokens via 4 transformer layers (hidden width 256, 4 attention heads). The **Envisioner** utilizes a hierarchical LLM: Qwen3-Omni serving as the high-level multimodal

backbone and Qwen3-0.6B as the low-level control backbone. The **Advancer** is a lightweight decoder-only transformer (4 layers, width 512, 8 heads) that predicts next-step Mimi audio codes from the semantic latent  $z_{t_k}$ . Finally, the **Realizer** generates qpos action chunks using a flow-matching action head with  $N_{\text{ODE}} = 8$  Euler integration steps.

Key training hyperparameters are standardized as follows:

- **Audio Processing:** Sample rate  $f_s = 16$  kHz; causal window length  $T_{\text{win}} = 4.0$  s (64,000 samples). To improve robustness against environmental and mechanical ego-noise, we augment training audio with additive noise (SNR uniformly sampled in  $[0, 20]$  dB) and random gain ( $[-6, +6]$  dB).
- **Optimization:** AdamW optimizer with a learning rate of  $1e-4$ , weight decay of 0.05, and a cosine decay schedule featuring a 5% linear warmup. Gradients are clipped at a maximum norm of 1.0.
- **Training Horizon:** 200k steps for OpenX-Sound pretraining, 50k steps per task for HEAR-Bench fine-tuning, and 30k steps per task for real-robot fine-tuning, utilizing a global batch size of 256 sequences.
- **Loss Weights:**  $w_{\text{adv}} = 0.1$  and  $w_{\text{text}} = 0.05$ , with a linear warm-up over the first 20% of the fine-tuning.

All models are trained and evaluated on an Ubuntu 22.04 workstation equipped with two NVIDIA RTX 5090 GPUs, utilizing PyTorch with CUDA. For real-robot experiments, the end-to-end latency  $\tau_{\text{sys}}$  is empirically estimated from timestamped sensing and command logs, whereas in simulation we default to  $\tau_{\text{sys}} = 0$  to explicitly isolate the execution gaps induced by action chunking.

**6.1.3 Baselines** To systematically evaluate the efficacy of the VSLA paradigm, we benchmark HEAR against broadly adopted VLA models and specialized audio-native policies. For a rigorous comparison, all baselines follow the identical two-stage training protocol, receive the same visual observations and causal audio segments, and output identical qpos action chunks.

**VLA Backbones and Audio Adapters.** We select **OpenVLA** (Kim et al. 2024) and  $\pi_{0.5}$  (Intelligence et al. 2025) as our representative VLA backbones. By default, these models are vision-only, relying solely on  $I_{t_k}^{1:V}$ ,  $l$ , and  $s_{\bar{t}_k}$ . To equip them with auditory capabilities, we implement two standard adapters. The **-Waveform** variant renders the causal 1D audio window  $A_{t_k}$  into a 2D line plot image, treating it as an additional camera view. While this approach captures amplitude envelopes and sudden acoustic onsets, it inherently collapses temporal dynamics into a static spatial

representation and discards fine-grained spectral frequencies. Conversely, the **-ASR** variant processes the audio through an Automatic Speech Recognition module, appending the resulting transcript to the language prompt. This approach effectively captures explicit verbal commands but discards critical non-speech acoustics and prosody.

*Compact Audio-Native Policies.* We also compare against **Play it by Ear** (Du et al. 2022) and **ManiWAV** (Liu et al. 2024b), two pioneering policies designed explicitly for audio-visual manipulation. These models natively ingest raw audio and benefit from fast inference rates, which theoretically allows for shorter decision intervals. However, their relatively compact parameter scale limits their capacity for long-horizon, compositional reasoning. Including these baselines allows us to demonstrate that processing audio natively is necessary but insufficient; robust sound-centric manipulation also requires the architectural capacity to maintain causal memory and perform complex multimodal reasoning across extended task horizons.

## 6.2 Simulation on HEAR-Bench

We rigorously evaluate our approach in simulation using HEAR-Bench (Section 5.2), built upon the dual-arm RoboTwin2 platform (Figure 6a). HEAR-Bench provides a streaming microphone signal and strictly enforces the sound-causal success rules defined in Eq. (10). The fundamental difficulty of this benchmark lies in bridging execution gaps without missing brief acoustic events, maintaining stable control during prolonged, visually quasi-static waiting phases, and understanding physical contact sounds.

**6.2.1 Task Suite and Design Rationale** We systematically design seven tasks in HEAR-Bench to cover a complementary taxonomy of sound-centric challenges (Table 2). Figures 7 through 13 provide representative qualitative key frames from HEAR rollouts in simulation.

- **Sustained trigger, Alarm Clock.** Tests indefinite waiting and suppressing visually plausible early actions until an auditory precondition is satisfied.
- **Impulse trigger, Microwave.** Tests capturing an extremely brief event that can occur inside an execution gap (especially the Blind Execution Interval under open-loop chunking), then acting after the cue has vanished.
- **Prosody, Check Yes.** Uses identical text but different intonation to force reasoning beyond ASR outputs.
- **Contact and materials, Check Materials.** Uses visually similar objects so the impact timbre serves as a low-cost proxy for physical property sensing.

- **Continuous monitoring, Pour Water and Boil Water.** Requires tracking gradual acoustic evolution over long horizons when vision is weak or static.
- **Random override, Interrupt.** Places a spoken interrupt at random times to discourage ignoring audio and to test safe mode switching mid-motion.

**6.2.2 Main Results** Table 3 reports the success rates over 100 trials per task. HEAR achieves the highest overall performance, demonstrating an average success rate of 81%. Among the VLA baselines, rendering a waveform as an image provides a moderate improvement for tasks with distinct volume spikes, whereas the ASR adapter primarily benefits tasks featuring explicit speech commands.

Notably, the compact audio-native policies, Play it by Ear and ManiWAV, outperform the vision-only backbones but generally trail behind the adapted VLA models and HEAR. Because these lightweight models run at higher inference rates, their performance gap is not primarily a runtime issue; rather, their limited architectural capacity makes long-horizon, multi-stage behaviors brittle and restricts robust generalization. As expected, vision-only policies struggle significantly across the suite, confirming that visual heuristics alone are insufficient for these sound-gated tasks. Furthermore, under an identical training protocol, OpenVLA and its variants consistently underperform  $\pi_{0.5}$  and its variants, underscoring that sound-centric closed-loop manipulation remains highly sensitive to backbone capacity and action modeling choices.

### 6.2.3 Trigger Tasks

*Alarm Clock.* For the *Alarm Clock* task, the robot is positioned in front of a clock whose stop button remains visible throughout the episode, as shown in Figure 7. The alarm begins ringing at a random time. The robot must keep both arms still until the ringing starts and press the button only after the onset, leaving arm selection to the policy. Pressing before the ring violates sound-causality and is counted as a failure under Eq. (10).

This setup is intentionally designed as a tempting shortcut. A vision-only policy can always see the button and may attempt to press it immediately, which would appear reasonable under standard goal-reaching metrics. Randomizing the onset time prevents fixed-delay heuristics and highlights the asynchronous nature of acoustic evidence. Because the onset can fall between inference cycles and be missed by a one-shot windowed audio interface, success requires robustness to temporal misalignment.

As shown in Table 3, HEAR achieves a 0.91 success rate. The best baseline is  $\pi_{0.5}$ -Waveform at 0.80, followed by

**Table 3. Simulation results on HEAR-Bench.** Success rates  $\uparrow$  are averaged over 100 independent trials per task. The “VLA” column indicates whether the baseline relies on a vision-language-action backbone.

Method	VLA	Alarm Clock	Check Yes	Check Materials	Pour Water	Boil Water	Microwave	Interrupt	Avg.
OpenVLA (Kim et al. 2024)	Y	0.00	0.33	0.31	0.00	0.00	0.00	0.03	0.10
OpenVLA-Waveform (Kim et al. 2024)	Y	0.71	0.60	0.63	0.26	0.37	0.45	0.69	0.53
OpenVLA-ASR (Kim et al. 2024)	Y	0.16	0.59	0.10	0.06	0.03	0.41	0.65	0.29
$\pi_{0.5}$ (Intelligence et al. 2025)	Y	0.00	0.48	0.43	0.00	0.00	0.00	0.09	0.14
$\pi_{0.5}$ -Waveform (Intelligence et al. 2025)	Y	0.80	0.73	0.71	0.31	0.43	0.52	0.75	0.61
$\pi_{0.5}$ -ASR (Intelligence et al. 2025)	Y	0.21	0.70	0.15	0.09	0.04	0.52	0.74	0.35
Play it by Ear (Du et al. 2022)	N	0.45	0.38	0.39	0.15	0.10	0.12	0.38	0.28
ManiWAV (Liu et al. 2024b)	N	0.40	0.31	0.41	0.12	0.17	0.08	0.32	0.26
<b>HEAR</b>	Y	<b>0.91</b>	<b>0.89</b>	<b>0.83</b>	<b>0.51</b>	<b>0.81</b>	<b>0.85</b>	<b>0.88</b>	<b>0.81</b>

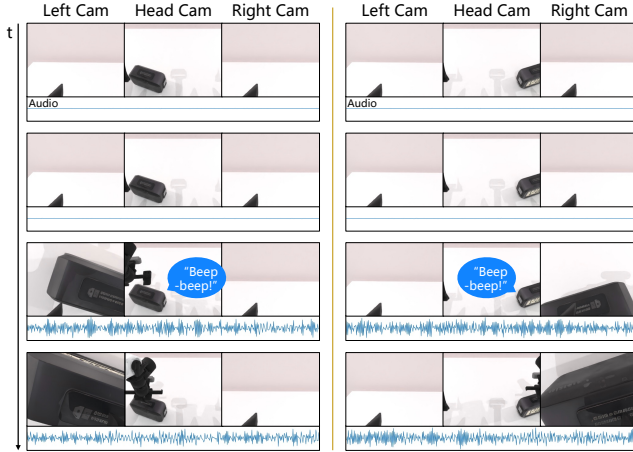


**Figure 7. Qualitative execution on HEAR-Bench: Alarm Clock.** The policy waits for the ring onset, autonomously selects an arm, and presses the stop button strictly after the acoustic cue. This prevents visually plausible but premature actions.

OpenVLA-Waveform at 0.71. ASR-based variants perform poorly since the cue is non-speech. Furthermore, as expected, vision-only policies struggle to complete these tasks, confirming that visual heuristics alone are insufficient when critical state transitions are acoustically gated. When baselines fail, the dominant error is an early press driven by visual affordances. Waveform rendering helps once the ring is fully present because the amplitude spike is visually obvious, but it often overfits to brittle threshold rules and remains sensitive to where the onset falls inside the rendered window. HEAR avoids these artifacts by encoding the raw 1D waveform and integrating onset evidence into a causal memory, allowing the policy to wait stably and commit only after the cue.

**Microwave.** The *Microwave* scenario requires the robot to stand by until the appliance emits a brief “ding” at a randomized time, as shown in Figure 8. The correct behavior is to open the door only after this transient cue has occurred.

This task is designed to directly stress cue dropout under execution gaps. The acoustic cue can be shorter than the effective perception-action gap  $G_k$  (Eq. (5)) and may occur while the policy is not being queried, such as inside

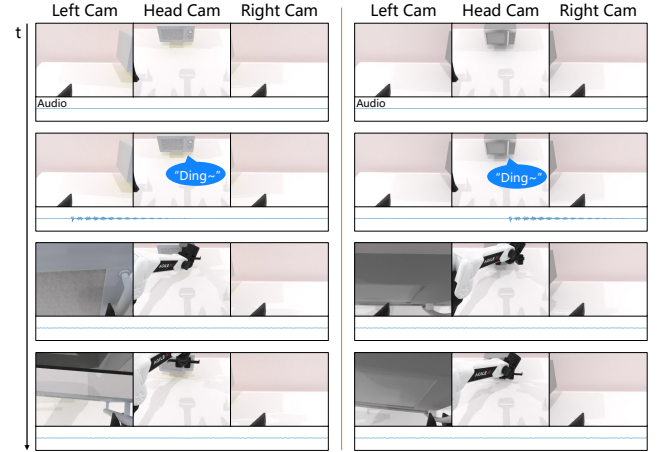


**Figure 8. Qualitative execution on HEAR-Bench: Microwave.** A brief “ding” occurs at a randomized time. The robot successfully captures this transient cue and opens the door only after the sound has finished.

the Blind Execution Interval under open-loop chunking (Section 3.2.3). By the next decision time, the cue may have already vanished from the most recent window  $A_t$ , making it unobservable to memoryless policies (Eq. (7)).

HEAR maintains a 0.85 success rate. The strongest baselines are  $\pi_{0.5}$ -Waveform and  $\pi_{0.5}$ -ASR, both reaching 0.52. Audio-native baselines also struggle, with Play it by Ear achieving 0.12 and ManiWAV achieving 0.08. This indicates that simply accepting audio as an input does not automatically resolve cue dropout under delayed updates. Waveform image rendering fails primarily by missing the short amplitude spike when it falls between visual frames, causing the robot to wait indefinitely. HEAR performs well because the Historizer module compresses transient evidence into a persistent causal memory state  $h_{t_k}$  (Eq. (8)), enabling correct actions even after the sound has ceased.

#### 6.2.4 Spoken Commands and Prosody

**Check Yes.** To evaluate prosody comprehension, *Check Yes* presents the robot with two identical bottles and requires it to identify the correct one, as shown in Figure 9. The episode is constructed so the robot first lifts the initial bottle and then receives spoken feedback that is lexically identical

but prosodically different. “Yes!” indicates affirmation, meaning the robot picked the correct bottle. “Yes?” indicates doubt, meaning it must switch to the other bottle.

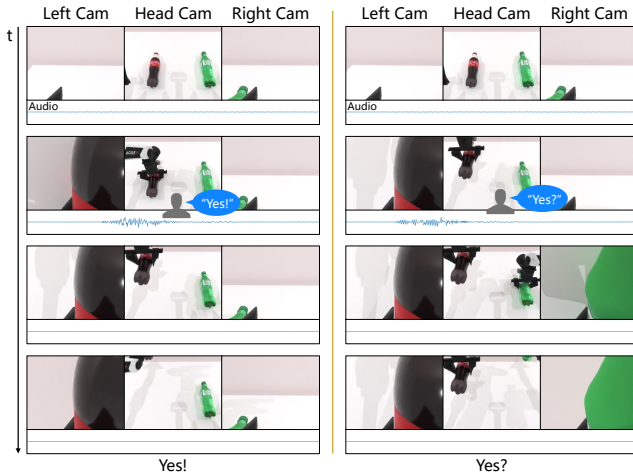


**Figure 9. Qualitative execution on HEAR-Bench: Check Yes.** The spoken transcript is consistently “Yes”. The robot relies entirely on intonation and prosody to determine whether to hold the current object or switch to the alternative.

This task requires speech understanding beyond basic transcripts. A pure ASR-to-text interface collapses both outcomes into near-identical token sequences, discarding the pragmatic intent. Robust success therefore benefits from modeling intonation directly from the waveform, a capability critical for real human-robot interaction where prosody can invert meaning.

HEAR reaches a 0.89 success rate. While ASR captures the lexical content, it compresses intonation into text, blurring the distinction between affirmation and doubt ( $\pi_{0.5}$ -ASR achieves 0.70). The waveform-as-image fails because pitch and prosody variations are largely invisible in a standard amplitude envelope plot. HEAR improves upon these baselines by learning a dedicated 1D waveform encoder that preserves prosody and fusing these features directly with vision, language, and proprioception.

*Interrupt.* Beyond understanding intent, robots must also respond to speech dynamically during execution. During the *Interrupt* evaluation, as illustrated in Figure 10, the robot initiates a standard manipulation routine, autonomously choosing which arm to use (Figure 10). At a random time mid-motion, a spoken “reset” command is issued. The correct response is to immediately terminate the current trajectory and return to the initial pose.

Because the interrupt timing is randomized, a purely visual policy that simply completes the routine will fail under sound-causality metrics. Furthermore, this task stresses action binding, as the same keyword must trigger different

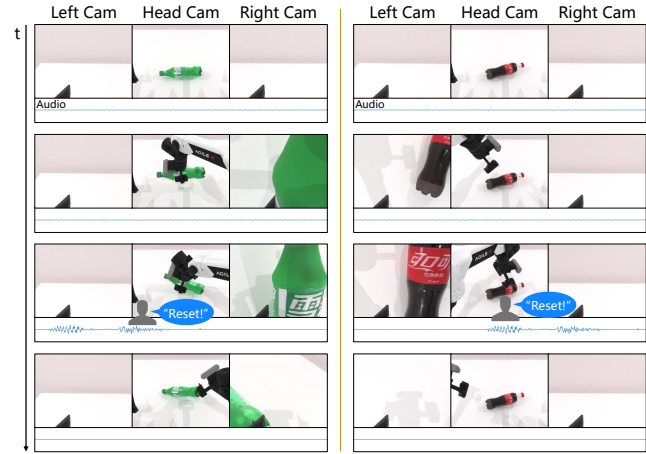


**Figure 10. Qualitative execution on HEAR-Bench: Interrupt.** While performing an ongoing manipulation routine, the robot receives a randomized spoken “reset” command. It immediately overrides its current motion and safely returns to the initial pose.

low-level control outputs depending on the robot’s current joint positions.

HEAR leads with a 0.88 success rate. Waveform and ASR baselines perform reasonably well (0.75 and 0.74 for  $\pi_{0.5}$ , respectively) because the cue is explicit speech. However, reacting safely under chunked control depends heavily on how the command is fused with the current motion state. HEAR improves robustness by integrating speech evidence into the same representation used for action chunk generation, producing smoother joint-position trajectories that minimize overshoot during abrupt course corrections.

### 6.2.5 Contact and Materials

*Check Materials.* As depicted in Figure 11, the *Check Materials* setup features two visually identical plates placed within the workspace. One plate is the target material, and the other is a distractor. The robot must pick up a cube, drop it onto the first plate to produce an impact sound, and infer from the audio whether it landed on the target material. If incorrect, it must move the cube to the second plate.

This task serves as a controlled example of using hearing as a low-cost physical sensor. Material properties often require tactile feedback to disambiguate when vision is aliased (Clarke et al. 2018). Here, we make vision intentionally uninformative to force reliance on contact timbre. Unlike *Alarm Clock*, the robot must actively generate informative audio and then deliberately hold still to listen, tightly coupling perception quality to control stability.

HEAR achieves a 0.83 success rate. ASR variants fail dramatically (0.15 for  $\pi_{0.5}$ -ASR) as they cannot convert impact acoustics into useful text. We observe two dominant issues in baseline failures. First, memoryless policies are sensitive to the exact placement of the brief impact within

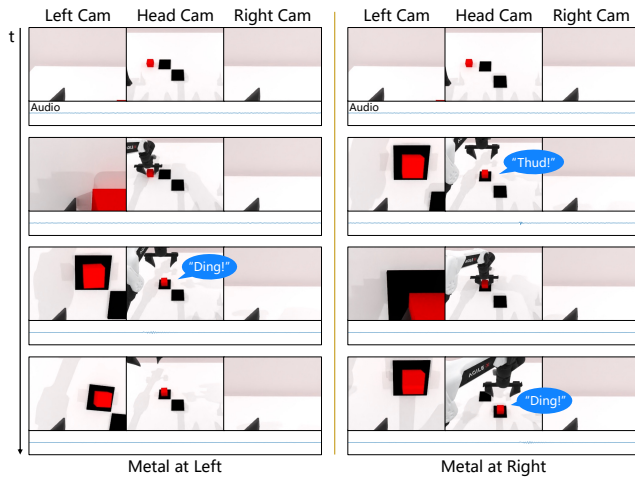


**Figure 11. Qualitative execution on HEAR-Bench: *Check Materials*.** The robot drops a cube onto one of two visually identical plates. It infers the underlying material property entirely from the resulting impact acoustics to complete the sorting task.

the observation window. Second, waveform images struggle to capture the subtle frequency differences (timbre) between materials, making the visual plot highly ambiguous. HEAR benefits from operating on the raw audio stream and retaining causal memory for the transient impact and smoother chunk generation through the Realizer module, which helps the robot pause deliberately and increases the effective signal-to-noise ratio.

### 6.2.6 Process Monitoring

*Pour Water.* When executing *Pour Water*, the robot dispenses liquid into an opaque container and must halt precisely at a target level specified by the language instruction, a process visualized in Figure 12. Since the fill level is visually occluded, the decision signal is the continuous evolution of the pouring sound.

We include this task to evaluate continuous temporal flow. The relevant information is not an isolated acoustic event but the rate and direction of change in sound over time. This challenges snapshot-style audio interfaces because adjacent observation windows can sound remarkably similar even as the correct control decision evolves.

HEAR reaches a 0.51 success rate, significantly outperforming  $\pi_{0.5}$ -Waveform (0.31). A visual plot of pouring noise often appears as a dense, static block of lines, making it difficult for a vision backbone to track gradual acoustic evolution. In HEAR, the Historizer aggregates evidence over time, but continuous processes also require sensitivity to progression. The Advancer module provides predictive dynamics supervision by predicting near-future acoustic tokens (Eq. (18) and (19)). This mechanism forces the fused representations to encode local temporal gradients, effectively

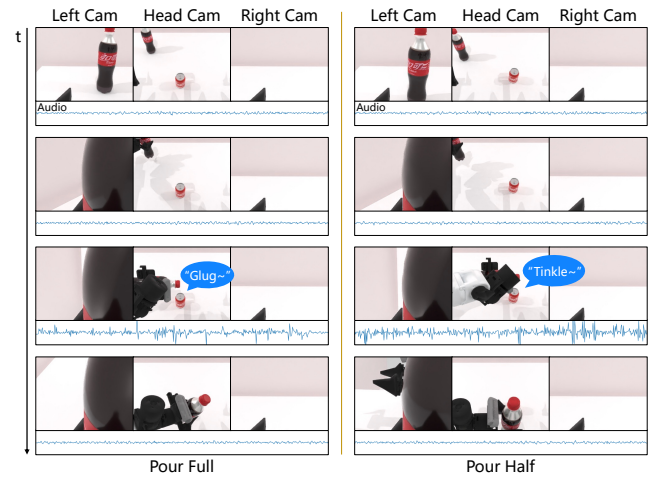


**Figure 12. Qualitative execution on HEAR-Bench: *Pour Water*.** The robot dispenses liquid into an opaque container and stops precisely at a target level guided by continuous acoustic feedback. The vertical axis of the audio waveform is scaled by 10x for visualization.

learning how the sound is changing over time rather than just recognizing what the sound is at a single instant.

*Boil Water.* Figure 13 demonstrates the *Boil Water* environment, which requires the robot to monitor a pot and intervene strictly once the acoustic profile indicates a rolling boil. The time-to-boil is randomized to prevent reliance on fixed waiting schedules.

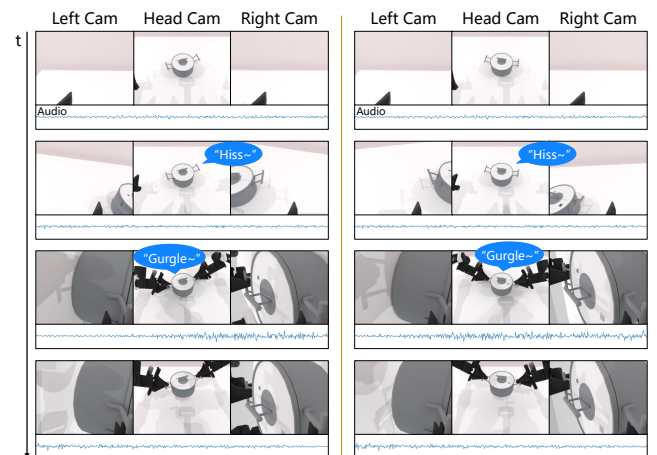


**Figure 13. Qualitative execution on HEAR-Bench: *Boil Water*.** The robot maintains a stable posture through a prolonged, visually static period and intervenes strictly once the evolving sound indicates a rolling boil. The vertical axis of the audio waveform is scaled by 10x for visualization.

This task isolates long waiting periods characterized by subtle acoustic transitions. The visual scene remains static while the sound evolves gradually from silence to a simmer, and finally to a sustained boil. Success requires the policy to remain still for an arbitrary duration and detect a sustained acoustic pattern rather than a transient burst.

HEAR achieves a 0.81 success rate, compared to 0.43 for  $\pi_{0.5}$ -Waveform. Baseline failures typically involve early actions triggered by visually plausible heuristics or overreactions to transient noisy bursts. HEAR mitigates these errors by smoothing short-term fluctuations through causal memory and tracking gradual acoustic progression via the predictive dynamics supervision in Advancer.

**6.2.7 Summary** Overall, HEAR demonstrates consistent improvements across diverse sound categories in HEAR-Bench. While waveform rendering serves as a strong baseline, it remains sensitive to window placement and lacks a principled mechanism for causal history. ASR is effective when cues can be cleanly tokenized into explicit speech, but it inherently discards non-speech details and prosody. HEAR succeeds across both discrete triggers and continuous processes because it treats the raw waveform as a first-class observation modality. By retaining salient evidence causally through the Historizer and learning progression-sensitive representations via the Advancer, the proposed architecture provides a robust foundation for audio-reactive robotic control.

## 6.3 Real-Robot Experiments

**6.3.1 Platform and Acoustic Challenges** We deploy the trained policies on a single-arm Franka Panda with two RGB views (head and arm cameras) and a single standard microphone placed near the workspace (Figure 6(b)). The policy observes the identical  $o_{t_k}$  interface defined in Eq. (4). We intentionally avoid specialized acoustic sensors such as contact microphones or ear-in-hand arrays, requiring the system to process raw, ambient acoustic signals.

Real-world audio introduces structural challenges absent in simulation, including room reverberation, non-stationary background noise, and device-specific acoustic variations. Additionally, the robot’s own physical motion generates mechanical ego-noise. These factors make stable waiting and deliberate, repeatable contact behaviors far more critical than in pristine simulated environments. All tasks are evaluated over 100 independent trials using the sound-causal success definitions outlined in Section 3.4.1.

**6.3.2 Task Suite and Design Rationale** We evaluate four real-world tasks that mirror the simulation requirements while explicitly introducing the complexities of physical acoustics. Figures 14–17 provide representative qualitative key frames.

- **Moka Coffee** (Long-horizon process monitoring). Requires waiting and reacting to subtle acoustic

phase changes with minimal visual progression. While previous robotic coffee-making demonstrations typically involve operating automated machines via discrete actions (e.g., pressing a button to dispense) (Fu et al. 2024), this task requires the robot to monitor the continuous, physical stovetop brewing process and make decisions based entirely on auditory feedback.

- **Answer Phone** (Multi-stage speech and events). Requires responding to a transient ring, understanding speech during a call, and using audio to determine when to end the interaction under severe visual aliasing (repeated visual states).
- **Shake Bottle** (Self-generated cue). Requires active motion to elicit sound for hidden-state classification, emphasizing the coupling between deliberate proprioception and acoustic perception.
- **Real Alarm Clock** (Sustained trigger). Tests robust waiting and reaction timing under acoustic domain shifts, including reverberation and background noise.

**6.3.3 Results** Table 4 reports the success rates across physical deployments. HEAR achieves a 0.54 average success rate across the four tasks. While moving from simulation to the real world introduces significant acoustic challenges, HEAR consistently outperforms all baselines. Rendering a waveform as an image remains the strongest VLA baseline (averaging 0.39 for  $\pi_{0.5}$ ), while the ASR adapter provides benefits primarily on explicit speech or sustained triggers.

The audio-native non-VLA policies, Play it by Ear and ManiWAV, struggle significantly in these complex real-world settings, averaging only 0.34. Although these compact policies can theoretically execute at higher frequencies, their smaller parameter scale makes them highly brittle to real-world acoustic variability and extended task horizons. Consistent with simulation findings, OpenVLA and its variants underperform  $\pi_{0.5}$  and its variants under the same training protocol.

### 6.3.4 Task Breakdown

**Moka Coffee.** For the *Moka Coffee* evaluation, the physical robot is stationed near a Moka pot and a serving cup, as shown in Figure 14. The brewing process proceeds for an extended period, during which the visual scene remains largely static. Because a traditional Moka pot lacks electronic sensors or discrete visual indicators of completion, the robot cannot rely on digital feedback or simple visual heuristics. Instead, the robot must remain still and monitor the evolving sound of the boiling water and steam. It must

**Table 4. Real-robot evaluation results.** Success rates  $\uparrow$  across four physical tasks, averaged over 100 trials each. All tasks strictly enforce the sound-causal success criteria, penalizing visually plausible but premature actions.

Method	VLA	Moka Coffee	Answer Phone	Shake Bottle	Real Alarm Clock	Avg.
OpenVLA (Kim et al. 2024)	Y	0.00	0.00	0.22	0.01	0.06
OpenVLA-Waveform (Kim et al. 2024)	Y	0.04	0.05	0.41	0.77	0.32
OpenVLA-ASR (Kim et al. 2024)	Y	0.01	0.01	0.19	0.63	0.21
$\pi_{0.5}$ (Intelligence et al. 2025)	Y	0.00	0.01	0.48	0.04	0.13
$\pi_{0.5}$ -Waveform (Intelligence et al. 2025)	Y	0.05	0.06	0.54	0.90	0.39
$\pi_{0.5}$ -ASR (Intelligence et al. 2025)	Y	0.01	0.02	0.21	0.78	0.26
Play it by Ear (Du et al. 2022)	N	0.04	0.06	0.42	0.85	0.34
ManiWAV (Liu et al. 2024b)	N	0.05	0.05	0.45	0.81	0.34
<b>HEAR</b>	Y	<b>0.18</b>	<b>0.15</b>	<b>0.88</b>	<b>0.96</b>	<b>0.54</b>

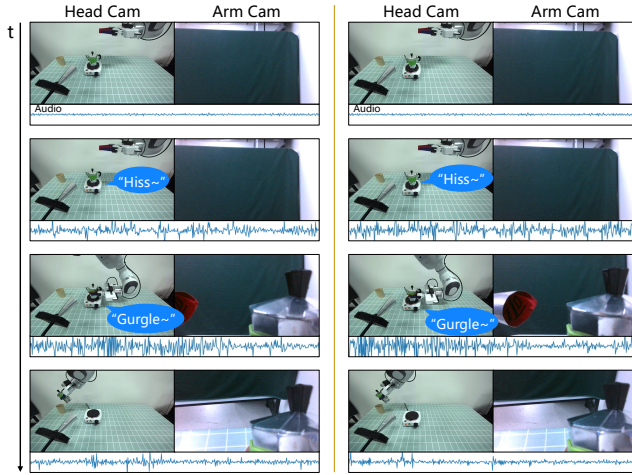


**Figure 14. Real-robot physical deployment: Moka Coffee.**

The robot monitors the complex acoustics of an uninstrumented Moka pot and initiates pouring only after detecting the characteristic sputtering phase. The vertical axis of the audio waveform is scaled by 10x for visualization.

grasp the pot and pour the coffee strictly after the acoustic profile transitions into the characteristic sputtering phase, which indicates that the extraction is complete. Pouring early is counted as a failure.

Because a traditional Moka pot lacks electronic sensors or discrete visual indicators of completion, the robot cannot rely on digital feedback or simple visual heuristics. Instead, the most reliable progress signal is acoustic. Success in this scenario requires the robot to make a sound-based judgment of an ongoing physical process, much like a human would.

Despite the inherent complexity of this task, HEAR achieves a 0.18 success rate. While this absolute performance highlights the extreme difficulty of long-horizon acoustic monitoring in unconstrained real-world environments, HEAR still provides a substantial improvement over the baselines. The strongest baseline,  $\pi_{0.5}$ -Waveform, drops to a 0.05 success rate, and audio-native policies like ManiWAV and Play it by Ear similarly collapse to 0.05 and 0.04, respectively. We observe that real-world mechanical ego-noise and ambient sounds severely disrupt mechanical methods. Waveform rendering often encourages

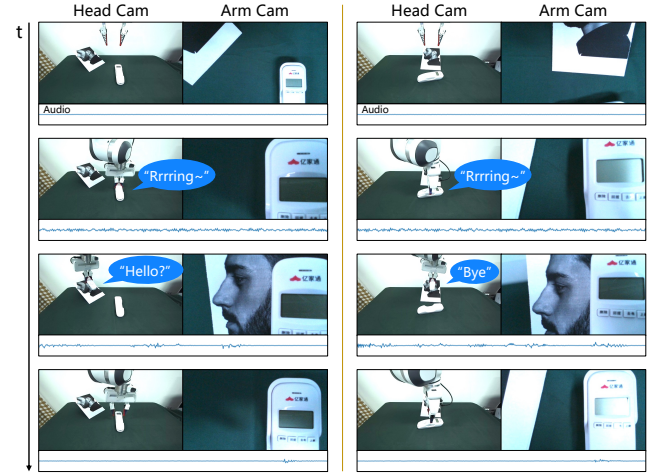


**Figure 15. Real-robot physical deployment: Answer Phone.**

Despite severe visual aliasing, the robot successfully waits for a ringtone, hands the phone to a user, and returns it to the base only after the acoustic end-of-call signal.

brittle amplitude-threshold heuristics, causing models to trigger too early on background noise spikes or miss the subtle transition phase entirely. HEAR navigates this challenging environment better by using causal audio memory and predictive dynamics supervision to track continuous temporal flow, though handling unconstrained real-world cooking acoustics remains an open challenge for future research.

*Answer Phone.* As shown in Figure 15, the *Answer Phone* sequence begins with the robot waiting for a randomized ringtone, after which it must retrieve a handset from a box and hand it to a person. During the call, it listens to speech. When the call ends, indicated by a hang-up sound or end-of-call speech, it must return the phone to the box.

This long-horizon task combines multiple sound categories and exposes severe visual aliasing. From a single RGB frame, the robot near the phone box looks nearly identical when it should pick up the ringing phone and when it should return the phone after a call. Correct behavior therefore depends entirely on progress tracking and causal history rather than snapshot visual recognition.

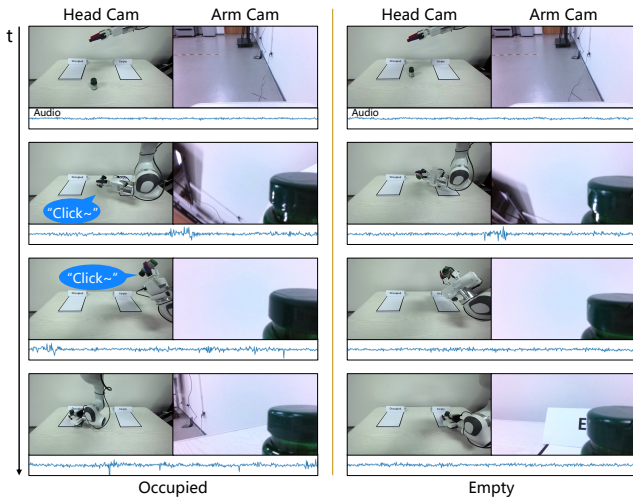


**Figure 16. Real-robot physical deployment: *Shake Bottle*.** The robot performs a deliberate shaking motion to actively elicit sound from an opaque bottle, using the resulting rattle to classify its hidden contents. The vertical axis of the audio waveform is scaled by 10x for visualization.

HEAR reaches a 0.15 success rate, significantly outperforming  $\pi_{0.5}$ -Waveform (0.06) and ManiWAV (0.05). This task proved exceptionally challenging due to the combination of severe visual aliasing and complex overlapping real-world audio. When baselines fail, they almost universally advance prematurely. For instance, they attempt to return the phone before the call ends or become paralyzed by the repeated visual frames. HEAR triples the success rate of the best baseline by leveraging the Envisioner’s progress representation and causal audio memory. This mechanism helps preserve brief end-of-call acoustic cues that are otherwise masked by speech, demonstrating the necessity of temporal memory even when overall task success remains difficult.

*Shake Bottle*. To test active acoustic sensing, *Shake Bottle* prompts the robot to grasp an opaque bottle and perform a brisk shaking motion to elicit sound. Based on the resulting rattle, the robot classifies the bottle as occupied or empty, as depicted in Figure 16. It then places the bottle into the corresponding region.

Unlike passive listening, this setup is a classic example of interactive perception. The acoustic evidence depends entirely on the robot’s own motion. The same bottle can sound quiet if the shake is too weak. Success demands coupling audition with proprioception and generating repeatable motion primitives.

HEAR reaches a 0.88 success rate. Waveform rendering remains the strongest baseline ( $\pi_{0.5}$ -Waveform at 0.54), while vision-only variants are weak (0.22 to 0.48). HEAR achieves this result by fusing audio directly with joint positions (qpos) and producing smoother, highly repeatable

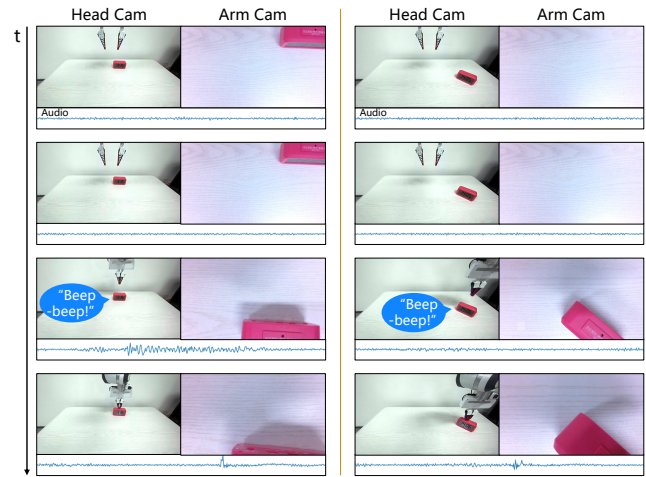


**Figure 17. Real-robot physical deployment: *Real Alarm Clock*.** Operating under real-world background noise, the robot suppresses early visual heuristics and presses the button strictly after the sustained ring begins. The vertical axis of the audio waveform is scaled by 10x for visualization.

shaking trajectories via the Realizer, ensuring the elicited acoustic evidence is consistent across trials.

*Real Alarm Clock*. Deploying the alarm scenario in the physical world, *Real Alarm Clock* features a device that produces a sustained ring at an unpredictable moment. Figure 17 demonstrates how this setup requires the robot to suppress early actions and press the button only after the acoustic onset.

This setting tests whether policies remain sound-causal under physical domain shifts, including room reverberation and background chatter, and whether they can suppress the visually tempting early-press shortcut.

HEAR reaches a 0.96 success rate. Waveform rendering performs robustly ( $\pi_{0.5}$ -Waveform achieves 0.90), and ASR variants are competitive on this sustained cue ( $\pi_{0.5}$ -ASR at 0.78). Vision-only baselines fail frequently (0.01 to 0.04). In failed baseline trials, waveform images are occasionally destabilized by room reverberation which alters the visual envelope, leading to threshold artifacts. The text interface of ASR inherently compresses temporal detail, making reaction timing less precise. HEAR remains highly reliable because it operates directly on waveform-derived embeddings and integrates evidence continuously, effectively eliminating premature presses and missed onsets despite the noisy physical environment.

#### 6.4 System Analysis and Ablations

We conduct extensive ablations in the HEAR-Bench simulation environment to isolate the mechanisms driving performance and to understand the underlying challenges of sound-centric manipulation. To ensure a fair comparison,

**Table 5. Component ablations in HEAR-Bench.** We report the average success rate across all seven simulation tasks, demonstrating the contribution of each architectural module and training phase.

Variant	Avg. success $\uparrow$
<b>HEAR full (OpenX-Sound pretrained)</b>	<b>0.81</b>
No OpenX-Sound pretraining	0.69
No Historizer	0.57
Historizer: causal GRU memory	0.67
Historizer: EMA/pooling memory	0.62
No Advancer	0.73
No stage text	0.77
No low-level controller	0.75
Realizer regression	0.70

**Table 6. Analysis of temporal motion collapse.** We report the fraction of low-motion steps (end-effector displacement  $< 2$  mm) across executed action sequences in simulation. Lower values  $\downarrow$  indicate smoother, more continuous motion without freezing.

Variant	Low-motion ratio $\downarrow$
<b>HEAR full (OpenX-Sound pretrained)</b>	<b>0.15</b>
No OpenX-Sound pretraining	0.18
No Historizer	0.29
Historizer: causal GRU memory	0.20
Historizer: EMA/pooling memory	0.22
No Advancer	0.33
No stage text	0.20
No low-level controller	0.24
Realizer regression	0.38

each ablation uses the same demonstrations, observation interface, and action representation, changing only the targeted component. Unless stated otherwise, we report the average task success rate over the seven simulation tasks based on 100 trials per task.

**6.4.1 Component Ablations** Table 5 isolates the contribution of individual architectural choices. First, removing the OpenX-Sound pretraining phase causes a substantial drop in average success (from 0.81 to 0.69). This indicates that large-scale audio-visual pretraining is important for stabilizing representation learning prior to task-specific fine-tuning, even when downstream evaluation occurs in simulation.

Removing the Historizer results in the most severe performance decline (dropping to 0.57). This supports our core premise that a causal memory mechanism is necessary to preserve transient acoustic evidence across discrete decision boundaries. We also tested lighter memory alternatives, such as a causal GRU (0.67) and an exponential moving average (EMA) pooling over audio features (0.62). While these improve upon a memoryless design, they remain noticeably below our Streaming Stateful Transformer (SST). This suggests that the additional capacity and streaming attention provided by SST translate directly to more robust sound-causal control.

Removing the Advancer by dropping the auxiliary acoustic-token prediction objective (Eq. (19)) reduces the average success to 0.73. The decline is most pronounced in continuous temporal flow tasks, where tracking the progression and rate of change is more critical than detecting a single discrete event. Similarly, removing stage text supervision or the low-level controller noticeably impacts tasks that require quick behavioral shifts. Finally, replacing the Realizer’s flow-matching head with direct regression lowers the average to 0.70. Jittery motion generated by straightforward regression injects mechanical self-noise into the microphone signal, obscuring brief cues and degrading both control quality and auditory sensing.

#### 6.4.2 Temporal Motion Collapse and Action Continuity

Chunked policies operating over long horizons can suffer from Temporal Motion Collapse, a phenomenon where meaningful movement is concentrated early in a chunk while later steps degenerate into near-identical actions (Intelligence et al. 2025; Zhao et al. 2023). To quantify this effect, we compute a Cartesian displacement diagnostic for the end-effector:  $d_t \triangleq \|p_{t+1} - p_t\|_2$ , where  $p_t$  is the position implied by the commanded joint angles at time  $t$ . We classify a step as “low-motion” if  $d_t < 2$  mm and report the fraction of such steps across all executed sequences in Table 6.

The full HEAR model exhibits the lowest fraction of degenerate steps (0.15). Removing the Advancer or replacing the Realizer with regression increases this ratio to 0.33 and 0.38, respectively. This diagnostic suggests that the predictive temporal grounding from the Advancer, paired with the smooth vector field generation of the Realizer, helps mitigate motion collapse. Consequently, the robot maintains stable and continuous behavior even during extended listening phases.

#### 6.4.3 Impact of Replanning Frequency

We investigate whether timing failures can be resolved by closing the control loop more frequently. To this end, we evaluate the trained HEAR policy under three execution wrappers during inference: (i) standard open-loop execution of the predicted chunk, (ii) executing the first action of the chunk and holding it for the remaining  $H - 1$  steps, and (iii) executing half of the chunk ( $H/2$  actions) before re-querying the policy.

As shown in Table 7, truncating chunks trades reactivity for stability. Executing half a chunk before re-querying yields only a marginal change compared to the default open-loop execution. However, executing and holding only a single action drastically alters behavior and reduces success to 0.71. More frequent re-querying does not eliminate the fundamental end-to-end system latency. In our rollouts,

**Table 7. Impact of replanning frequency.** We evaluate a fixed HEAR checkpoint under different chunk-execution strategies. Aggressive replanning (e.g., executing only the first action) degrades performance, highlighting that simply increasing the query rate cannot replace causal memory.

Execution strategy	Avg. success $\uparrow$
Execute only the first action	0.71
Execute only the first half of each chunk ( $H/2$ )	0.80
<b>Open-loop chunk execution (default)</b>	<b>0.81</b>

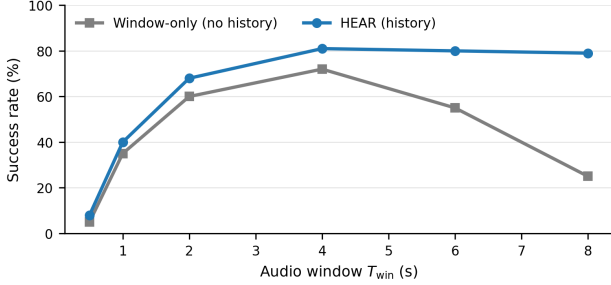


**Figure 18. Sensitivity to audio window length.** Average success rate  $\uparrow$  on HEAR-Bench across different per-query audio window durations ( $T_{win}$ ). Memoryless adapters show a rise-then-fall performance trend, whereas HEAR improves and then remains stable due to its causal memory.

aggressive replanning tends to introduce chunk-to-chunk discontinuities. This stop-and-go behavior generates ego-noise that can mask subtle cues precisely when the robot is attempting to listen. This analysis highlights that simply replanning faster is not a free substitute for causal memory.

**6.4.4 Sensitivity to Window Length and Execution Gaps** Windowed audio interfaces introduce a delicate hyperparameter in the form of the window duration  $T_{win}$ . As illustrated in Figure 18, memoryless adapters like waveforms and ASR exhibit a non-monotonic trend. If the window is too short, brief cues are missed. If it is too long, distinct interaction phases blur together, which encourages the policy to learn brittle timing heuristics. In contrast, HEAR improves and then plateaus as the window grows, because its causal memory integrates history beyond a single snapshot.

Furthermore, we stress-test the system’s resilience to execution gaps by varying the chunk horizon  $H_{exec}$  at inference time, keeping the trained weights fixed (Figure 19). As  $H_{exec}$  increases, the open-loop decision interval widens. Memoryless windowed baselines experience significant cue dropout, consistent with the evidence-vanishing condition formalized in Eq. (7). HEAR remains substantially more stable across large execution gaps. This isolates the benefit of decoupling the high-frequency auditory sensing cadence from the lower-frequency decision cadence.

**6.4.5 Failure Modes and Error Signatures** Across evaluations, memoryless baselines predominantly suffer from two distinct failure modes. The first is acting early, where the

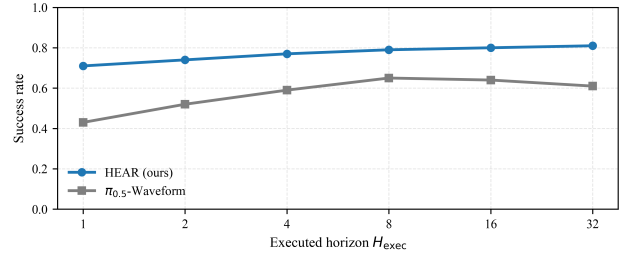


**Figure 19. Sensitivity to execution gaps.** Average success rate  $\uparrow$  as the executed chunk horizon ( $H_{exec}$ ) increases. Window-only baselines suffer from severe cue dropout under large execution gaps, while HEAR remains highly robust.

**Table 8. Error mode decomposition.** We report the average false-trigger (acting prematurely) and miss-detection (failing to act after a cue) rates on HEAR-Bench. HEAR effectively mitigates both failure modes compared to vision-only and memoryless baselines.

Method	Avg. FT $\downarrow$	Avg. MD $\downarrow$
OpenVLA (Kim et al. 2024)	0.91	0.57
OpenVLA-Waveform (Kim et al. 2024)	0.15	0.18
OpenVLA-ASR (Kim et al. 2024)	0.46	0.21
$\pi_{0.5}$ (Intelligence et al. 2025)	0.89	0.52
$\pi_{0.5}$ -Waveform (Intelligence et al. 2025)	0.12	0.11
$\pi_{0.5}$ -ASR (Intelligence et al. 2025)	0.41	0.17
Play it by Ear (Du et al. 2022)	0.38	0.10
ManiWAV (Liu et al. 2024b)	0.31	0.09
<b>HEAR</b>	<b>0.02</b>	<b>0.04</b>

robot commits to a plausible action based on vision alone, violating sound causality. The second is susceptibility to execution gaps, where a brief cue occurs between decisions and becomes unobservable by the next query.

To make these errors measurable, we define the false-trigger rate (acting before the required sound cue) and the miss rate (failing to act after the cue). Using the timestamps from Eq. (10), a trial is a false trigger if  $t_{goal} < t_{snd}$ , and a miss if  $t_{snd} \leq T < t_{goal}$ . Table 8 shows that vision-only models fail almost exclusively through false triggers (e.g., 0.91 for OpenVLA). Waveform adapters reduce false triggers but still exhibit notable miss rates when cues misalign with the observation window. HEAR effectively mitigates both error modes.

Finally, the ablations reveal distinct error signatures that highlight the coupling of perception and control. Without the Historizer, failures on trigger tasks typically manifest as “miss then wait”; the robot never commits because the cue vanished during an execution gap. Without the Advancer, continuous flow tasks tend to fail late, with the robot continuing to pour or wait after the sound has progressed. Replacing the Realizer with regression increases small oscillations, which raises self-noise and triggers spurious reactions. Together, these patterned reinforce a core principle

of sound-centric manipulation: a policy that listens while moving must also move in ways that make listening possible.

## 7 Discussion and Future Work

The introduction of the Vision-Sound-Language-Action (VSLA) paradigm provides a useful perspective on multi-sensory robot learning. While modern vision-language-action models have achieved remarkable success by relying on persistent visual states, our findings suggest that robust physical interaction often requires robots to process transient environmental signals in real time. In this section, we reflect on the broader implications of our framework, acknowledge current system limitations, and outline potential directions for audio-driven robotics.

### 7.1 Broader Implications for Multisensory Control

The core structural challenge addressed by HEAR extends beyond just audio processing. It reflects a universal tension in modern robot systems between high-frequency, transient sensory events and low-frequency, delayed policy updates. In typical manipulation environments, visual states degrade gracefully under system delay because objects generally remain in the camera’s view. Acoustic events, however, are highly ephemeral. A brief impact sound or a completion beep can easily occur and vanish within a single open-loop action chunk, rendering it completely unobservable to memoryless control policies.

Our work demonstrates that simply appending new sensory modalities to existing VLA architectures is insufficient. When dealing with transient signals under inevitable end-to-end system latency, robust closed-loop control requires deliberate architectural design. Specifically, it necessitates decoupling the high-frequency sensing cadence from the lower-frequency decision cadence. By utilizing a continuous causal memory to bridge execution gaps and introducing predictive dynamics to ground the policy in the flow of time, HEAR prevents critical information loss. We believe this system-level principle will become increasingly relevant not only for auditory perception but also for integrating other high-frequency, physical modalities into large-scale foundation models. For instance, recent efforts to unlock physical knowledge through tactile sensing face similar challenges regarding the transient nature of contact forces (Huang et al. 2025). Designing architectures that maintain causal persistence across execution gaps will be essential for fully realizing the potential of these diverse sensory inputs.

### 7.2 The Data Bottleneck in Audio-Driven Robotics

Scaling the VSLA paradigm naturally encounters a severe lack of synchronized, real-world audio data in existing robot learning datasets. While our OpenX-Sound dataset provides a scalable workaround by synthesizing temporally aligned audio from video, we must explicitly acknowledge the domain gap this introduces. Advanced video-to-audio generation models can produce perceptually plausible soundscapes, but they do not perfectly capture true physical acoustics. Generated audio may occasionally omit subtle contact cues, alter precise event timings, or hallucinate sounds that lack a true physical source.

Because sound-centric tasks are highly sensitive to causality and timing, these synthetic artifacts limit the ceiling of purely offline pretraining. Consequently, OpenX-Sound serves primarily as a bootstrapping mechanism for representation learning rather than a complete substitute for physical data. Moving forward, the robotics community would benefit from collecting native datasets that include synchronized microphone recordings alongside standard metadata, such as microphone placement and room acoustic properties. Until such datasets become widely available, fine-tuning on real-world, task-specific demonstrations remains a necessary step for reliable physical deployment.

### 7.3 Limitations and Future Directions

While our approach provides a concrete step toward sound-centric manipulation, the current system has several limitations that open exciting avenues for future work.

First, our hardware setup relies on a single workspace microphone. This configuration inherently limits the robot’s ability to localize sound sources or reliably separate overlapping acoustic events in noisy environments, a challenge functionally similar to the classic cocktail party problem (Cherry 1953). Future systems could benefit from spatial hearing capabilities by integrating multi-microphone arrays, such as combining a base microphone with an end-effector microphone. This would provide spatial acoustic cues and improve signal-to-noise ratios through active beamforming.

Second, our policies are trained entirely via offline imitation learning. Consequently, the robot’s robustness is strictly bounded by the diversity of acoustic noise and timing variations present in the demonstration data. Real-world deployment introduces unpredictable mechanical ego-noise and unmodeled room reverberations that can easily degrade perception. Exploring online fine-tuning or reinforcement

learning methods that allow the robot to adapt to its specific acoustic environment on the hardware would significantly enhance deployment reliability (Lu et al. 2025).

Finally, our current observation interface processes audio and vision as distinct streams before fusing them at the representation level. In human perception, however, subtle visual micro-motions are often deeply synchronized with sound generation. Future architectures might explore native audio-visual video encoders that process synchronized multimodal clips directly (Kim et al. 2026). This integration could help robots better associate specific acoustic timbres with physical contact events, further reducing visual aliasing and paving the way for more holistic physical intelligence.

## 8 Conclusion

This paper formalized the Vision-Sound-Language-Action (VSLA) paradigm to overcome the fundamental limitations of vision-centric robot policies in sound-dependent environments. We identified that the primary bottleneck in audio-driven manipulation is the temporal mismatch between transient acoustic cues and the delayed, chunked execution loops of modern VLA systems. To resolve this, we proposed HEAR, an architecture that decouples high-frequency auditory perception from low-frequency decision-making. By integrating a streaming causal memory and predictive temporal grounding, HEAR effectively bridges execution blind spots to enable reliable, closed-loop physical reactions.

To support policy learning and rigorous evaluation, we introduced the OpenX-Sound pretraining dataset alongside HEAR-Bench, enforcing strict sound-causal success criteria. Extensive evaluations demonstrated the efficacy of our approach, with HEAR achieving an 81% average success rate in simulation and 54% across diverse real-world deployments on a physical robot. Ultimately, our results establish that incorporating audio into foundation models requires more than simply appending an input stream; it demands persistent causal memory and explicit temporal alignment. We hope the VSLA paradigm and our accompanying open-source tools provide a reliable foundation for advancing fully embodied, multi-sensory intelligence.

## References

- Ahn M, Brohan A, Brown N, Chebotar Y, Cortes O, David B, Finn C, Fu C, Gopalakrishnan K, Hausman K et al. (2023) Do as i can, not as i say: Grounding language in robotic affordances. In: *Proceedings of The 6th Conference on Robot Learning, Proceedings of Machine Learning Research*, volume 205. PMLR, pp. 287–318.
- Arandjelovic R and Zisserman A (2017) Look, Listen and Learn. In: *Proceedings of the IEEE International Conference on Computer Vision*. pp. 609–617.
- Baevski A, Zhou Y, Mohamed A and Auli M (2020) wav2vec 2.0: A Framework for Self-Supervised Learning of Speech Representations. In: *Advances in Neural Information Processing Systems*, volume 33. pp. 12449–12460.
- Brohan A, Brown N, Carbajal J, Chebotar Y, Dabis J, Finn C, Gopalakrishnan K, Hausman K, Herzog A, Hsu J et al. (2023) RT-1: Robotics Transformer for Real-World Control at Scale. In: *Proceedings of Robotics: Science and Systems*.
- Chen C, Jain U, Schissler C, Gari SVA, Al-Halah Z, Ithapu VK, Robinson P and Grauman K (2020) SoundSpaces: Audio-Visual Navigation in 3D Environments. In: *European Conference on Computer Vision*. Springer, pp. 17–36.
- Chen S, Wu Y, Wang C, Liu S, Tompkins D, Chen Z and Wei F (2023) Beats: Audio pre-training with acoustic tokenizers. In: *Proceedings of the 40th International Conference on Machine Learning, Proceedings of Machine Learning Research*, volume 202. PMLR, pp. 5178–5193.
- Chen T, Chen Z, Chen B, Cai Z, Liu Y, Li Z, Liang Q, Lin X, Ge Y, Gu Z et al. (2025) RobotWin 2.0: A Scalable Data Generator and Benchmark with Strong Domain Randomization for Robust Bimanual Robotic Manipulation. *arXiv preprint arXiv:2506.18088*.
- Cherry EC (1953) Some Experiments on the Recognition of Speech, with One and with Two Ears. *Journal of the Acoustical Society of America* 25: 975–979.
- Chi C, Xu Z, Feng S, Cousineau E, Du Y, Burchfiel B, Tedrake R and Song S (2025) Diffusion Policy: Visuomotor Policy Learning via Action Diffusion. *The International Journal of Robotics Research* 44(10-11): 1684–1704.
- Clarke S, Rhodes T, Atkeson CG and Kroemer O (2018) Learning audio feedback for estimating amount and flow of granular material. In: *Proceedings of The 2nd Conference on Robot Learning, Proceedings of Machine Learning Research*, volume 87. PMLR, pp. 529–550.
- Défossez A, Mazaré L, Orsini M, Royer A, Pérez P, Jégou H, Grave E and Zeghidour N (2024) Moshi: A Speech-Text Foundation Model for Real-Time Dialogue. *arXiv preprint arXiv:2410.00037*.
- Deng T, Chen Y, Zhang L, Yang J, Yuan S, Liu J, Wang D, Wang H and Chen W (2024) Compact 3d gaussian splatting for dense visual slam. *arXiv preprint arXiv:2403.11247*.
- Deng T, Pan Y, Yuan S, Li D, Wang C, Li M, Chen L, Xie L, Wang D, Wang J, Civera J, Wang H and Chen W (2025) What is the best 3d scene representation for robotics? from geometric to foundation models. *arXiv preprint arXiv:2512.03422*.

- Driess D, Xia F, Sajjadi MS, Lynch C, Chowdhery A, Ichter B, Wahid A, Tompson J, Vuong Q, Yu T et al. (2023) PaLM-E: An Embodied Multimodal Language Model. In: *Proceedings of the 40th International Conference on Machine Learning, Proceedings of Machine Learning Research*, volume 202. PMLR, pp. 8469–8488.
- Du M, Lee OY, Nair S and Finn C (2022) Play It by Ear: Learning Skills Amidst Occlusion Through Audio-Visual Imitation Learning. In: *Proceedings of Robotics: Science and Systems*.
- Elizalde B, Deshmukh S, Al Ismail M and Wang H (2023) CLAP: Learning Audio Concepts from Natural Language Supervision. In: *ICASSP 2023-2023 IEEE International Conference on Acoustics, Speech and Signal Processing (ICASSP)*. IEEE, pp. 1–5.
- Fu Z, Zhao TZ and Finn C (2024) Mobile aloha: Learning bimanual mobile manipulation with low-cost whole-body teleoperation. *arXiv preprint arXiv:2401.02117*.
- Girdhar R, El-Nouby A, Liu Z, Singh M, Alwala KV, Joulin A and Misra I (2023) ImageBind: One Embedding Space to Bind Them All. In: *Proceedings of the IEEE/CVF Conference on Computer Vision and Pattern Recognition*. pp. 15180–15190.
- Gong Y, Chung YA and Glass J (2021) AST: Audio Spectrogram Transformer. In: *Interspeech*. pp. 571–575.
- Gu J, Xiang F, Li X, Ling Z, Liu X, Mu T, Tang Y, Tao S, Wei X, Yao Y et al. (2023) Maniskill2: A unified benchmark for generalizable manipulation skills. In: *International Conference on Learning Representations*.
- Guo D, Liu H and Sun F (2023) Audio–Visual Language Instruction Understanding for Robotic Sorting. *Robotics and Autonomous Systems* 159: 104271.
- Guo H, Wang S, Ma R, Jiang S, Ghasempour Y, Abari O, Guo B and Qiu L (2025) OmniVLA: Physically-Grounded Multimodal VLA with Unified Multi-Sensor Perception for Robotic Manipulation. *arXiv preprint arXiv:2511.01210*.
- Heess N, Hunt JJ, Lillicrap TP and Silver D (2015) Memory-Based Control with Recurrent Neural Networks. *arXiv preprint arXiv:1512.04455*.
- Huang J, Wang S, Lin F, Hu Y, Wen C and Gao Y (2025) Tactile-VLA: Unlocking Vision-Language-Action Model’s Physical Knowledge for Tactile Generalization. *arXiv preprint arXiv:2507.09160*.
- Huang W, Wang C, Zhang R, Li Y, Wu J and Fei-Fei L (2023) Voxposer: Composable 3d value maps for robotic manipulation with language models. In: *Proceedings of The 7th Conference on Robot Learning, Proceedings of Machine Learning Research*, volume 229. PMLR, pp. 540–562.
- Intelligence P, Black K, Brown N, Darpinian J, Dhabalia K, Driess D, Esmail A, Equi M, Finn C, Fusai N et al. (2025)  $\pi_{0.5}$ : a vision-language-action model with open-world generalization. In: *arXiv preprint arXiv:2504.16054*.
- Jaderberg M, Mnih V, Czarnecki WM, Schaul T, Leibo JZ, Silver D and Kavukcuoglu K (2017) Reinforcement Learning with Unsupervised Auxiliary Tasks. In: *International Conference on Learning Representations*.
- James S, Ma Z, Arrojo DR and Davison AJ (2020) RL Bench: The Robot Learning Benchmark & Learning Environment. *IEEE Robotics and Automation Letters* 5(2): 3019–3026.
- Jones J, Mees O, Sferrazza C, Stachowicz K, Abbeel P and Levine S (2025) Beyond Sight: Finetuning Generalist Robot Policies with Heterogeneous Sensors via Language Grounding. In: *2025 IEEE International Conference on Robotics and Automation (ICRA)*. IEEE, pp. 5961–5968.
- Kim MJ, Gao Y, Lin TY, Lin YC, Ge Y, Lam G, Liang P, Song S, Liu MY, Finn C et al. (2026) Cosmos Policy: Fine-Tuning Video Models for Visuomotor Control and Planning. *arXiv preprint arXiv:2601.16163*.
- Kim MJ, Pertsch K, Karamcheti S, Xiao T, Balakrishna A, Nair S, Rafailov R, Foster E, Lam G, Sanketi P et al. (2024) Openvla: An open-source vision-language-action model. In: *Proceedings of The 8th Conference on Robot Learning, Proceedings of Machine Learning Research*, volume 270. PMLR, pp. 2679–2713.
- Kim S, Shukla A and Billard A (2014) Catching objects in flight. *IEEE Transactions on Robotics* 30(5): 1049–1065.
- Li H, Zhang Y, Zhu J, Wang S, Lee MA, Xu H, Adelson E, Fei-Fei L, Gao R and Wu J (2022) See, Hear, and Feel: Smart Sensory Fusion for Robotic Manipulation. In: *Proceedings of The 6th Conference on Robot Learning, Proceedings of Machine Learning Research*, volume 205. PMLR, pp. 1368–1378.
- Li L, Fan J, Ni X, Qin S, Li W and Gao F (2025) SVA: Towards Speech-Enabled Vision-Language-Action Model. *Pattern Recognition* : 112915.
- Lipman Y, Chen RT, Ben-Hamu H, Nickel M and Le M (2023) Flow Matching for Generative Modeling. In: *International Conference on Learning Representations*.
- Liu X, Gong C and Liu Q (2023) Flow Straight and Fast: Learning to Generate and Transfer Data with Rectified Flow. In: *International Conference on Learning Representations*.
- Liu X, Su K and Shlizerman E (2024a) Tell What You Hear From What You See – Video to Audio Generation Through Text. In: *Advances in Neural Information Processing Systems*, volume 37. pp. 101337–101366.
- Liu Z, Chi C, Cousineau E, Kuppuswamy N, Burchfiel B and Song S (2024b) Maniway: Learning robot manipulation from in-the-wild audio-visual data. In: *Proceedings of The 8th Conference on Robot Learning, Proceedings of Machine Learning Research*.

- Learning Research*, volume 270. PMLR, pp. 947–962.
- Liu Z, Liu J, Xu J, Han N, Gu C, Chen H, Zhou K, Zhang R, Hsieh KC, Wu K et al. (2025) MLA: A Multisensory Language-Action Model for Multimodal Understanding and Forecasting in Robotic Manipulation. *arXiv preprint arXiv:2509.26642* .
- Lu G, Guo W, Zhang C, Zhou Y, Jiang H, Gao Z, Tang Y and Wang Z (2025) VLA-RL: Towards Masterful and General Robotic Manipulation with Scalable Reinforcement Learning. *arXiv preprint arXiv:2505.18719* .
- Lu S and Culbertson H (2023) Active Acoustic Sensing for Robot Manipulation. In: *2023 IEEE/RSJ International Conference on Intelligent Robots and Systems (IROS)*. IEEE, pp. 3161–3168.
- Luo S, Yan C, Hu C and Zhao H (2023) Diff-Foley: Synchronized Video-to-Audio Synthesis with Latent Diffusion Models. In: *Advances in Neural Information Processing Systems*, volume 36. pp. 48855–48876.
- Mejia J, Dean V, Hellebrekers T and Gupta A (2024) Hearing Touch: Audio-Visual Pretraining for Contact-Rich Manipulation. In: *2024 IEEE International Conference on Robotics and Automation (ICRA)*. IEEE, pp. 6912–6919.
- Nakahara K and Calandra R (2025) Learning Gentle Grasping Using Vision, Sound, and Touch. In: *2025 IEEE/RSJ International Conference on Intelligent Robots and Systems (IROS)*. IEEE, pp. 7607–7614.
- Nie C, Wang G, Lie Z and Wang H (2025) Ermv: Editing 4d robotic multi-view images to enhance embodied agents. *arXiv preprint arXiv:2507.17462* .
- O'Neill A, Rehman A, Maddukuri A, Gupta A, Padalkar A, Lee A, Pooley A, Gupta A, Mandlekar A, Jain A et al. (2024) Open X-Embodiment: Robotic Learning Datasets and RT-X Models. In: *2024 IEEE International Conference on Robotics and Automation (ICRA)*. IEEE, pp. 6892–6903. DOI:10.1109/ICRA57147.2024.10611477.
- Perez E, Strub F, De Vries H, Dumoulin V and Courville A (2018) FiLM: Visual Reasoning with a General Conditioning Layer. In: *Proceedings of the AAAI Conference on Artificial Intelligence*, volume 32.
- Radford A, Kim JW, Xu T, Brockman G, McLeavey C and Sutskever I (2023) Robust Speech Recognition via Large-Scale Weak Supervision. In: *Proceedings of the 40th International Conference on Machine Learning, Proceedings of Machine Learning Research*, volume 202. PMLR, pp. 28492–28518.
- Sinapov J, Schenck C, Staley K, Sukhoy V and Stoytchev A (2014) Grounding Semantic Categories in Behavioral Interactions: Experiments with 100 Objects. *Robotics and Autonomous Systems* 62(5): 632–645.
- Sinapov J, Wiemer M and Stoytchev A (2009) Interactive Learning of the Acoustic Properties of Household Objects. In: *2009 IEEE International Conference on Robotics and Automation*. IEEE, pp. 2518–2524.
- Stein BE and Meredith MA (1993) *The merging of the senses*. MIT press.
- Team OM, Ghosh D, Walke H, Pertsch K, Black K, Mees O, Dasari S, Hejna J, Kreiman T, Xu C et al. (2024) Octo: An Open-Source Generalist Robot Policy. In: *Proceedings of Robotics: Science and Systems*. Delft, Netherlands.
- Wall V, Zöllner G and Brock O (2023) Passive and Active Acoustic Sensing for Soft Pneumatic Actuators. *The International Journal of Robotics Research* 42(3): 108–122.
- Wang R, Geng H, Li T, Wang F, Anumanchipalli G, Darrell T, Li B, Abbeel P, Malik J and Efros AA (2025a) The Sound of Simulation: Learning Multimodal Sim-to-Real Robot Policies with Generative Audio. *arXiv preprint arXiv:2507.02864* .
- Wang S, Fu J, Liu F, He X, Wu H, Shi J, Huang K, Fei Z, Gong J, Wu Z et al. (2025b) RoboOmni: Proactive Robot Manipulation in Omni-Modal Context. *arXiv preprint arXiv:2510.23763* .
- Wei X, Zhang H, Cao X, Xie S, Ge W, Li Y and Wang C (2025) Audio-VLA: Adding Contact Audio Perception to Vision-Language-Action Model for Robotic Manipulation. *arXiv preprint arXiv:2511.09958* .
- Xu J, Guo Z, Hu H, Chu Y, Wang X, He J, Wang Y, Shi X, He T, Zhu X et al. (2025) Qwen3-Omni Technical Report. *arXiv preprint arXiv:2509.17765* .
- Yang A, Li A, Yang B, Zhang B, Hui B, Zheng B, Yu B, Gao C, Huang C, Lv C et al. (2025) Qwen3 Technical Report. *arXiv preprint arXiv:2505.09388* .
- Zhang K, Kim DG, Chang ET, Liang HH, He Z, Lampo K, Wu P, Kymissis I and Ciocarlie M (2025) VibeCheck: Using Active Acoustic Tactile Sensing for Contact-Rich Manipulation. *arXiv preprint arXiv:2504.15535* .
- Zhao TZ, Kumar V, Levine S and Finn C (2023) Learning Fine-Grained Bimanual Manipulation with Low-Cost Hardware. In: *Proceedings of Robotics: Science and Systems*.
- Zhao W, Ding P, Zhang M, Gong Z, Bai S, Zhao H and Wang D (2025) VLAS: Vision-Language-Action Model with Speech Instructions for Customized Robot Manipulation. *arXiv preprint arXiv:2502.13508* .
- Zitkovich B, Yu T, Xu S, Xu P, Xiao T, Xia F, Wu J, Wohlhart P, Welker S, Wahid A et al. (2023) RT-2: Vision-Language-Action Models Transfer Web Knowledge to Robotic Control. In: *Proceedings of The 7th Conference on Robot Learning, Proceedings of Machine Learning Research*, volume 229. PMLR, pp. 2165–2183.